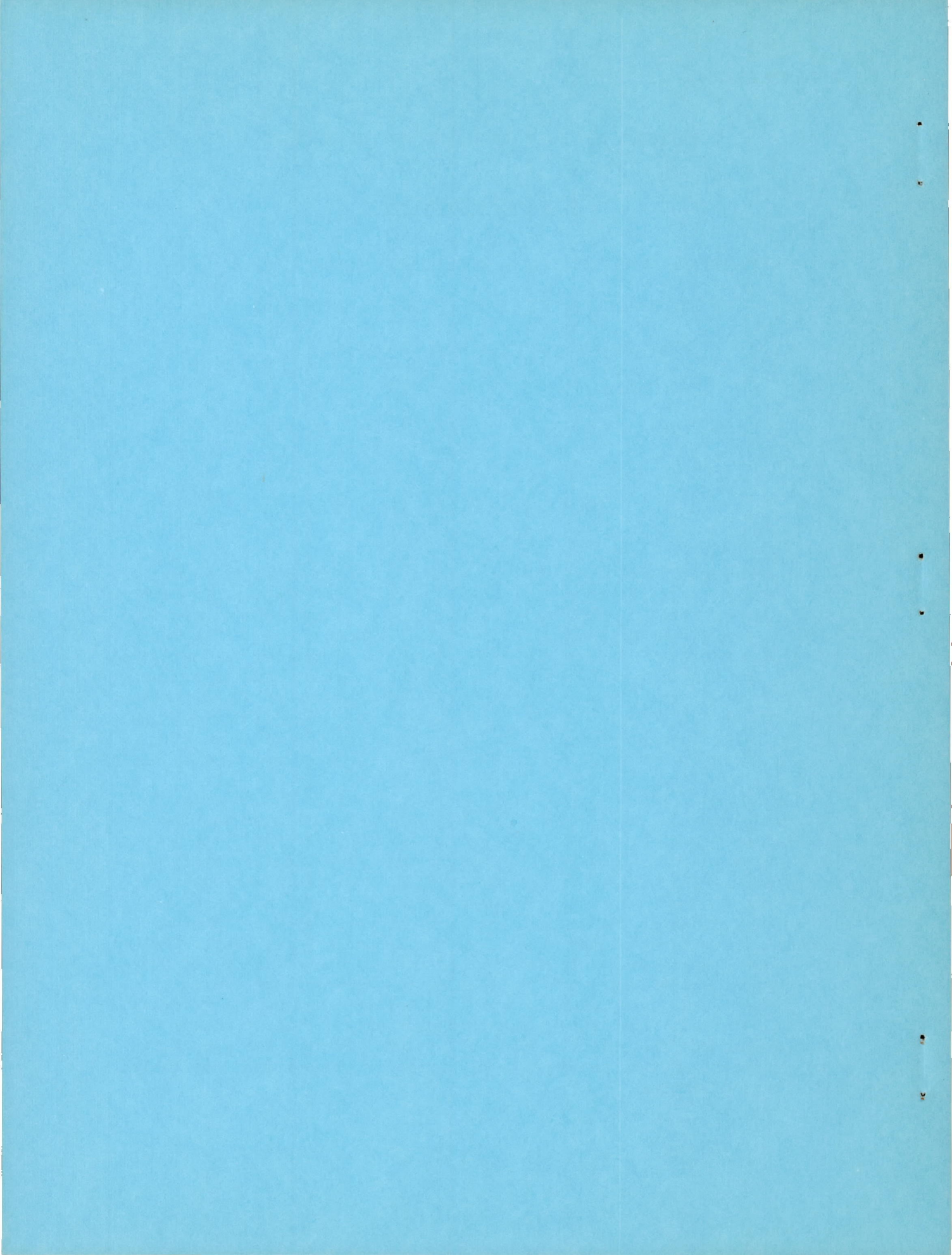# NACA

RESEARCH MEMORANDUM

WIND-TUNNEL INVESTIGATION AT MACH NUMBERS FROM 0.50

TO 1.29 OF AN UNSWEPT TAPERED WING OF ASPECT RATIO

2.67 WITH LEADING- AND TRAILING-EDGE FLAPS -

TRAILING-EDGE FLAPS DEFLECTED

By Louis S. Stivers, Jr., and Alexander W. Malick

Ames Aeronautical Laboratory
Moffett Field, Calif.

NATIONAL ADVISORY COMMITTEE
FOR AERONAUTICS

WASHINGTON

NATIONAL ADVISORY COMMITTEE FOR AERONAUTICS

RESEARCH MEMORANDUM

WIND-TUNNEL INVESTIGATION AT MACH NUMBERS FROM 0.50 TO 1.29

OF AN UNSWEPT TAPERED WING OF ASPECT RATIO 2.67

WITH LEADING- AND TRAILING-EDGE FLAPS -

TRAILING-EDGE FLAPS DEFLECTED

By Louis S. Stivers, Jr., and Alexander W. Malick

SUMMARY

Aerodynamic characteristics of an unswept wing having an aspect
ratio of 2.67, a taper ratio of 0.5, and employing full-span, 25-percent
chord, plain, trailing-edge flaps have been determined from wind-tunnel
tests of a semispan model. Sections of the wing model were 0.08 chord
thick from the 0.25- to the 0.75-chord points, and tapered to sharp lead-
ing and trailing edges. The data were obtained for a range of angles of
attack from -3° to 12° and for a range of trailing-edge-flap deflections
from -10° to 60° at Mach numbers from about 0.50 to 0.98 and from 1.09
to 1.29. The Reynolds number varied from about 0.94×10^6 to 1.27×10^6.
Whenever feasible the experimental results have been compared with theory.

In general, the trailing-edge flap was effective in changing the
lift coefficient at each angle of attack and Mach number of the investi-
gation. At the highest subsonic Mach numbers, however, small regions of
ineffectiveness or of negative effectiveness were evident at small flap
deflections. The effects of the flap-wing gaps at the lowest subsonic
Mach numbers were to increase the drag coefficients and decrease the
lift coefficients at the highest angles of attack. At the higher Mach
numbers, the effects of the gaps were, for the most part, small. Rela-
tively small variations with Mach number of the rate of change of flap-
hinge-moment coefficient with flap deflection were evident except at
Mach numbers near unity where comparatively large changes and reversals
in sign occurred. The effect of Mach number on the rate of change of
hinge-moment coefficient with angle of attack, however, was generally
much greater than that on the rate of change of hinge-moment coefficient
with flap deflection.

INTRODUCTION

Two significant problems associated with the application of low-aspect-ratio unswept wings to aircraft designed to operate at supersonic or high subsonic Mach numbers are (1) the improvement of the inherently low lift coefficients of such wings in landing or certain maneuvering attitudes, and (2) the selection of control surfaces that will be sufficiently effective throughout the range of flight Mach numbers. As a solution to these problems for wings having sharp-leading-edge airfoil sections, it has been proposed to employ both leading- and trailing-edge control surfaces. The aerodynamic characteristics of some unswept, low-aspect-ratio wings employing such control surfaces are reported in references 1 to 6. Except for reference 5, control-surface hinge-moment characteristics were not presented in these reports. Only in reference 6 are aerodynamic characteristics presented for both subsonic and supersonic Mach numbers.

To supplement the available information regarding the effectiveness and hinge-moment characteristics of leading- and trailing-edge control surfaces on low-aspect-ratio wings, an investigation has been made in the Ames 1- by 3-1/2-foot high-speed wind tunnel of a semispan model of an unswept, tapered wing of aspect ratio 2.67 equipped with full-span, 0.25 chord, plain, leading- and trailing-edge flaps. It is the purpose of this report to present the aerodynamic characteristics of the wing with the leading-edge flap undeflected and with the trailing-edge flap deflected. The characteristics are presented for Mach numbers from approximately 0.50 to 0.98 and from 1.09 to 1.29, with corresponding Reynolds numbers varying from about 0.94×10^6 to 1.27×10^6. Insofar as feasible, the experimental results are compared with theory.

NOTATION

c wing chord measured in streamwise direction

$\bar{c}$ mean aerodynamic chord of wing $\left(\dfrac{\int c^2 dy}{\int c \, dy} \right)$

C_D drag coefficient

$C_{D_{min}}$ minimum drag coefficient

C_{h_f} hinge-moment coefficient of trailing-edge flap
$$\left(\frac{\text{trailing-edge flap hinge moment}}{2q \text{ moment about hinge line of flap area behind hinge line}} \right)$$

$\dfrac{dC_{h_f}}{d\alpha}$ rate of change of hinge–moment coefficient with angle of attack, per degree

$\dfrac{dC_{h_f}}{d\delta_f}$ rate of change of hinge–moment coefficient with trailing–edge flap deflection, per degree

C_L lift coefficient

C_m pitching–moment coefficient about lateral axis through quarter–chord point of mean aerodynamic chord with mean aerodynamic chord as reference length

L/D lift–drag ratio

q free–stream dynamic pressure

R Reynolds number based on mean aerodynamic chord

y spanwise distance measured from wing–root–chord line

α wing angle of attack, degrees

α' wing geometric angle of attack, uncorrected for wind–tunnel jet–boundary interference (equivalent to α at supersonic Mach numbers), degrees

δ_f trailing–edge flap deflection, measured in plane normal to hinge line (positive when trailing edge is below chord plane), degrees

$\dfrac{d\alpha}{d\delta_f}$ trailing–edge flap–effectiveness parameter, absolute value of the ratio of the equivalent change in angle of attack to change in flap deflection at a constant lift coefficient

DESCRIPTION OF APPARATUS

The tests were conducted in the Ames 1– by 3–1/2–foot high–speed wind tunnel, a closed–throat tunnel vented to the atmosphere in the settling chamber. For the investigation the tunnel was equipped with a flexible–throat assembly (fig. 1) to permit operation at various subsonic and supersonic Mach numbers.

The model employed in the investigation was a semispan model of a complete wing having an aspect ratio of 2.67, a taper ratio of 0.5, and an unswept 50–percent chord line. The wing model was equipped with full–span, 25–percent chord, plain, leading– and trailing–edge flaps, the

hinge axes of which were coincident with the 25- and 75-percent chord lines of the wing. Sections of the wing in the streamwise direction were 0.08 chord thick from the 0.25 to the 0.75 chord points tapering to sharp leading and trailing edges. The included wedge angles of the flap sections were 18.2°. Plan and section views of the wing model together with the principal dimensions are shown in figure 2. The model was constructed of tool steel, hardened, ground, and polished. The leading- and trailing-edge radii were approximately 0.002 inch. The flaps were constructed with a 0.40-inch-diameter spindle attached at the root, such that the axes of the spindles were colinear with the hinge axes of the flaps. The spindles were fitted with electrical resistance strain gages of the torsion type for measuring the hinge moments of the flaps. Gaps of approximately 1/32 inch existed between the flaps and the wing panel.

The wing model was mounted on an 18-inch-diameter balance plate in the tunnel sidewall, as shown in the photograph of figure 3. Approximately 1/32-inch gaps existed between the roots of the undeflected flaps and the balance plate. The flap spindles extended through 1/2-inch-diameter holes in the plate. The face of the balance plate exposed to the tunnel air stream was flush with the tunnel wall, and an approximately 1/16-inch annular gap existed between the periphery of the plate and the tunnel wall. An external pressure-tight housing prevented flow through this gap from the outside atmosphere. Electrical resistance strain gages were fitted to the supports of the balance plate for measuring the reactions on the model. Lateral restraint was accomplished in such a manner that friction in a plane parallel to the balance-plate face was effectively eliminated.

TESTS

Lift, drag, and pitching moments of the wing, and hinge moments of the trailing-edge flap were determined as a function of Mach number for constant geometric angles of attack from -3° to 12° and for trailing-edge flap deflections of -10°, 0°, 20°, 40°, and 60°, with the flap-wing gaps unsealed. Except for flap deflections of 20° and 40°, lift, drag, and pitching moments were also obtained with the gaps sealed. The tests at small angles of attack for the undeflected flap were made at Mach numbers ranging from about 0.50 to 0.98 and from 1.09 to 1.29. No tests of the wing could be made at Mach numbers between 0.98 and 1.09 because of choking conditions in the tunnel test section. Reynolds numbers based on the mean aerodynamic chord of the wing varied from approximately 0.94×10^6 at a Mach number of 0.50 to approximately 1.27×10^6 at a Mach number of 1.15, as shown in figure 4.

CORRECTIONS TO DATA

The corrections to the angles of attack and drag coefficients of the wing due to wind–tunnel–wall interference at subsonic Mach numbers were determined from reference 7 and are indicated in reference 8 to be independent of Mach number. The wall–interference corrections (additive) which were applied to the data are as follows:

$$\Delta\alpha \text{ (deg)} = 0.51 \, C_L$$

$$\Delta C_D = 0.0089 \, C_L^2$$

All the data at subsonic Mach numbers have been corrected for model and wake blockage by the methods of reference 9. These blockage corrections vary with measured drag coefficient but are small for the most part, never exceeding a value of 3 percent even for the highest drag coefficients.

Tare corrections obtained with the model supported independently of the balance plate have been applied to the data at all the Mach numbers. These corrections were found to be practically independent of angle of attack or flap deflection and are given in coefficient form as follows:

M	Lift	Drag	Pitching Moment
0.50	0.018	0.031	0.006
.70	.015	.031	.004
.80	.014	.031	.003
.90	.013	.031	.001
.95	.017	.033	−.003
1.09	.001	.020	0
1.20	.005	.025	−.002
1.29	.003	.021	−.001

The pitching–moment data were obtained from the lift and drag reactions and are subject to combined errors of both the lift and drag measurements. Accordingly, in the present report, the pitching–moment coefficients are regarded as being of qualitative rather than quantitative significance.

The stream inclination at the model position was found to be sufficiently small for all the test Mach numbers that no stream–angle corrections were necessary.

Tunnel–wall boundary–layer measurements made at Mach numbers from 0.50 to 1.20 with the wind tunnel empty have indicated the existence of a stable, turbulent boundary layer with a displacement thickness of

0.12 inch at each Mach number. The velocity in the boundary layer at
each Mach number varied approximately as the 1/10 power of the distance
from the wall. The effect of possible drainage of low-energy air from
the tunnel-wall boundary layer by the low, induced pressures on the
wing is not known.

The effects of the possible flow of air around the flap-spindle
gaps and through the gap between the balance plate and the tunnel wall
are also unknown, but are believed to have been negligible.

RESULTS AND DISCUSSION

The basic force and moment data for the wing with undeflected
flaps, gaps unsealed and sealed, and hinge-moment data for the undeflec-
ted trailing-edge flap, gaps unsealed, are presented in graphical form.
The corresponding basic data for the wing with the trailing-edge flap
deflected are given in tables I to V.

Lift Characteristics

Lift coefficients for the wing with flap undeflected are shown in
figure 5 as a function of Mach number for various geometric angles of
attack. It can be observed in this figure that the only significant
changes in lift coefficient with increase in Mach number are the
increases for angles of attack of 9° and 12° at subsonic Mach numbers
above about 0.85. The variations with Mach number of the lift coeffi-
cients for the wing with the flap deflected (data given in tables I to V)
are similar to that for the wing with flap undeflected. The variations
are, in most instances, somewhat greater for the wing with flap deflected
than with flap undeflected. Sealing the gaps had generally little
effect on the variation of lift coefficient with Mach number.

Lift coefficients as a function of angle of attack with flap
deflection as a parameter are presented in figure 6. It is observed in
this figure that for the unsealed-gap configuration and for Mach num-
bers up to 0.90 the slopes of the lift curves at the highest angles of
attack are markedly lower than the slopes at zero angle of attack;
whereas for the higher Mach numbers the lift-curve slopes are practi-
cally a constant throughout the entire angle-of-attack range. The
effect of sealing the gaps was to increase noticeably the lift coef-
ficients at the highest angles of attack for Mach numbers up to 0.90.
Very little effect, however, is evident for the higher Mach numbers. It
is also apparent in this figure that at the smaller angles of attack the
lift-curve slopes for the wing with undeflected flaps at Mach numbers

from 0.80 to 1.09, gaps unsealed or sealed, are lower than those for the wing with flaps deflected. The lower lift-curve slope is believed to have resulted from separation of the flow over both surfaces of the trailing-edge flap by virtue of the large trailing-edge angle. This separation also adversely affected the hinge-moment and pitching-moment characteristics of the wing with undeflected flaps, as mentioned later in the discussion. Furthermore, it is noted that no reduction in the lift-curve slope of a wing with undeflected control surface is evident in the semispan-model data of reference 4 (obtained at a constant Reynolds number of 2.0×10^6), even for Mach numbers as high as 0.94. The trailing-edge angle of the model of this reference was only 5.1° as compared with 18.2° for the model of the present report.

The variations of lift coefficient with flap deflection for a constant angle of attack are shown in figure 7. In general, it may be seen that the trailing-edge flap is effective in changing the lift coefficient for each angle of attack and Mach number. Local regions of ineffectiveness, or of negative effectiveness, may be observed at the highest subsonic Mach numbers for the positive angles of attack at small negative flap deflections and for the negative angle of attack at small positive flap deflections. The effect of the gaps on the variation of lift coefficient with flap deflection was small, except at a Mach number of 0.50 and at the highest angles of attack for the higher subsonic Mach numbers. At a Mach number of 0.50 the rate of change of lift coefficient with flap deflection was noticeably increased by sealing the gaps.

The effect of Mach number on the lift-curve slope $dC_L/d\alpha$ near zero angle of attack is exhibited in figure 8 for the wing with undeflected flaps. Calculated values of the lift-curve slope for subsonic and supersonic Mach numbers were determined by the methods of references 10 and 11, respectively, and are also shown in this figure. Because of the particular geometry of the wing of the present investigation, the methods of the latter reference are applicable only for Mach numbers of 1.25 and greater.

It is observed in figure 8 that the effect of Mach number on the experimental lift-curve slopes was significant only at the highest subsonic Mach numbers. Sealing the gaps had, for the most part, only a small effect on the lift-curve slopes. It is apparent that the experimental lift-curve slope is considerably lower than that calculated. Such a disagreement might be expected in view of the large leading- and trailing-edge angles of the 8-percent-thick wing sections. Although the effect of Mach number on the calculated and experimental lift-curve slopes appears to be in agreement for Mach numbers up to 0.85, it is believed that such agreement for the present case is fortuitous.

The effect of Mach number on the flap-effectiveness parameter $d\alpha/d\delta_f$ at lift coefficients of 0, 0.2, and 0.4 is shown in figure 9.

Also shown in this figure for a lift coefficient of zero are theoretical
values of $d\alpha/d\delta_f$ for Mach numbers above 1.25, which were determined
using the expression for lift given in reference 11. For the calcula-
tions, the hinge line of the flap was swept ahead of the Mach line, and
it was assumed that the lift produced by flap deflection was independent
of the lift produced by the incidence of the wing. Accordingly, the
rate of change of lift coefficient with flap deflection was equal to the
lift-curve slope of a wing having the same plan form as the flap.

It is evident in figure 9 that for the subsonic Mach numbers the
values of $d\alpha/d\delta_f$ generally decrease with increase in Mach number. The
amount of the decrease, however, becomes smaller for successively greater
lift coefficients. At the supersonic Mach numbers the effect of Mach
number on the flap-effectiveness parameter was small. Only small changes
in the value of the parameter are evident for changes in lift coefficient.
It may also be seen in figure 9 that the effect of sealing the gaps was
significant only at the lowest subsonic Mach numbers. At these Mach
numbers, the flap-effectiveness parameter was markedly increased by
sealing the gaps. This increase resulted primarily from an increase in
the rate of change of lift coefficient with flap deflection. (See
fig. 7.) For Mach numbers between 1.25 and 1.29, it can be observed
that the experimental values of the flap-effectiveness parameter at zero
lift are about 0.6 of the calculated. Good agreement would not be
expected in view of differences noted in the experimental and calculated
lift characteristics.

<center>Hinge-Moment Characteristics</center>

The effect of Mach number on the hinge-moment coefficient of the
undeflected trailing-edge flap for various angles of attack is shown
in figure 10. Important variations of hinge-moment coefficient with
Mach number are evident for angles of attack up to 6° at Mach numbers
greater than about 0.85. For angles of attack of 9° and 12° the varia-
tions of hinge-moment coefficient are considerably different from those
for the lower angles. It is also noted that for angles of attack as
high as 6° the sign of the hinge-moment coefficients changes at Mach
numbers between 0.80 and 0.90, and again, for angles of attack of 3°
and 6°, at Mach numbers between 1.10 and 1.20. The asymmetry of the
curves about the zero hinge-moment axis, and the fact that the hinge-
moment coefficients are not equal to zero at zero angle of attack for
both the subsonic and supersonic Mach numbers are believed to be due to
a slight misalinement of the flap with the wing panel and to small errors
in setting the flap-deflection angle. The variations with Mach number
of the hinge-moment coefficient for the various flap deflections are
large, and the effects of changes in angle of attack are more uniform
for the deflected flap than for the undeflected flap. (See tables I to V.)

Hinge—moment coefficients for the flap as a function of angle of attack and of flap deflection are presented in figures 11 and 12, respectively. It is observed in figure 11 that the variations of hinge—moment coefficient with angle of attack are generally irregular at the subsonic Mach numbers for the smaller flap deflections. In figure 12 it is seen that the variations of hinge—moment coefficient with flap deflection are, for the most part, irregular at the smallest flap deflections for each Mach number except 1.29. Evidences of flap overbalance may be seen in some of the low angle—of—attack curves for Mach numbers of 0.90 and 0.95. In general, for flap deflections greater than about 20°, it is observed that at Mach numbers up to 0.90 the rate of change of hinge—moment coefficient with flap deflection is nearly constant.

The effects of Mach number on the rates of change of hinge—moment coefficient with angle of attack and with flap deflection are shown in figure 13. A substantial variation of $dC_{h_f}/d\alpha$ with Mach number is evident at the subsonic Mach numbers for the 0°, 10°, and 20° flap deflections, and at the supersonic Mach numbers up to about 1.20 for the —10°, 0°, and 20° flap deflections. Marked changes in the values of $dC_{h_f}/d\alpha$ with flap deflection are also apparent, especially at the subsonic Mach numbers. The positive value of $dC_{h_f}/d\alpha$ for the —10° flap deflection, which is found only at the subsonic Mach numbers, appears to be inconsistent with the corresponding data for the other deflections. The reason for this discrepancy is unknown. It can be observed that the value of $dC_{h_f}/d\alpha$ for the undeflected flap changes from negative to positive between Mach numbers of 0.85 and 0.90 and back to negative between Mach numbers of 1.10 and 1.15. It is believed that this undesirable hinge—moment characteristic is attributable to the large trailing—edge angle of the flap. This belief is substantiated by evidence reported in reference 12.

It can also be seen in figure 13 that the variation of $dC_{h_f}/d\delta_f$ with Mach number is small at Mach numbers up to about 0.70, but is significant at Mach numbers near unity. These variations of $dC_{h_f}/d\delta_f$, however, are observed to be considerably less than those of $dC_{h_f}/d\alpha$ with Mach number or with flap deflection. The values of $dC_{h_f}/d\delta_f$ at the highest subsonic Mach numbers become less negative with increase in Mach number for angles of attack as high as 6° and even become slightly positive for angles of attack of —3° and 0°. Both these effects are believed to result from the large trailing—edge angle of the flap. (See reference 12.)

Drag Characteristics

Drag coefficients for the wing with undeflected flaps are shown in figure 14 as a function of Mach number for various geometric angles of attack. It is observed in this figure that the variation of drag coefficient with Mach number is relatively unaffected by sealing the gaps. The effect of the gap on the minimum drag coefficients is shown in figure 15, where minimum drag coefficient is presented as a function of Mach number. It may be seen that for the subsonic Mach numbers the minimum drag coefficient for the wing with unsealed gaps is greater than that for the wing with sealed gaps, and the increment between the two appears to be nearly constant. At the supersonic Mach numbers the minimum drag coefficient for the wing with unsealed gaps is less than that for the wing with sealed gaps.

Drag coefficient as a function of lift coefficient with flap deflection as a parameter is shown in figure 16 for several Mach numbers. The effect of the gaps is the most pronounced at the highest lift coefficients shown for each flap deflection. At these lift coefficients the drag coefficients for the wing with sealed gaps are, in general, lower than those for the wing with unsealed gaps. For the 60° flap deflection the drag coefficients at the highest lift coefficients shown are markedly lower for the sealed-gap configuration.

Drag coefficient as a function of flap deflection with geometric angle of attack as a parameter is shown for the unsealed-gap configuration in figure 17. In this figure, it is observed that for each Mach number very large increases in the drag coefficient result from deflections of the flap. In general, the increase appears to be affected very little by angle of attack or by Mach number.

Lift-Drag Ratio Characteristics

The variation of lift-drag ratio with lift coefficient for the positive flap deflections is illustrated in figure 18. It may be seen in this figure that the maximum lift-drag ratio at each Mach number corresponds to either the 0° or 10° flap deflection. At the highest lift coefficients shown, the maximum ratios correspond to flap deflections of 10° or greater. As the lift coefficient is increased above approximately 0.4 the maximum lift-drag ratio is realized for successively greater flap deflections and is decreased in magnitude. The decrease can be seen to be much greater for the subsonic Mach numbers than for the supersonic Mach numbers. It is also observed in figure 18 that sealing the gaps generally increased the lift-drag ratios for each

flap deflection and Mach number, but this increase is significant only for the 0° and 10° flap deflections and for Mach numbers of about 0.80 or less.

Pitching-Moment Characteristics

Pitching-moment coefficients of the wing with undeflected flaps are presented in figure 19 as a function of Mach number for various geometric angles of attack. It is observed that sealing the gaps had very little effect on the variation of pitching-moment coefficient with Mach number. Pitching-moment coefficients as a function of lift coefficient with flap deflection as a parameter are shown in figure 20. In this figure it may be seen that the variations of pitching-moment coefficient with lift coefficient are generally irregular and do not appear to be materially affected by sealing the gaps. The pitching-moment coefficients of the wing for each flap deflection generally increase negatively for an increase in lift coefficient at each Mach number, except those for the wing with undeflected flap at the highest subsonic Mach numbers.

The variation of pitching-moment coefficient with flap deflection for the wing with unsealed gaps is presented in figure 21 for various angles of attack. Irregular variations are evident in this figure at the subsonic Mach numbers, especially for the smallest flap deflections. At the supersonic Mach numbers, nearly uniform variations are observed for the range of flap deflections shown, −10° to 20°.

The effect of Mach number on the center-of-pressure location at zero lift is shown in figure 22 for the wing with undeflected flaps. The corresponding calculated locations, also shown in this figure, were determined by the methods of references 10 and 11 for the subsonic and supersonic Mach numbers, respectively. Because of the geometry of the wing, the methods of reference 11 were not applicable for Mach numbers less than 1.25.

It may be seen in figure 22 that at the subsonic Mach numbers the experimental center-of-pressure locations for the wing with unsealed or sealed gaps lie near the calculated locations. From the pitching-moment data of figure 20 at the subsonic Mach numbers, it is evident that for the wing with deflected flaps the center-of-pressure location would be substantially behind that calculated for the undeflected flap. At the supersonic Mach numbers between 1.25 and 1.29, the experimental locations of the center of pressure are considerably forward of those calculated. It would appear from the pitching-moment data of figure 20 that for Mach numbers of 1.20 and 1.29 the locations of the center of pressure would be practically unchanged by flap deflection from −10° to 20°.

CONCLUSIONS

A semispan model of an unswept, tapered wing of aspect ratio 2.67 employing trailing-edge flaps and having sharp-leading-edge airfoil sections with a thickness-chord ratio of 0.08 has been investigated at Mach numbers from about 0.50 to 0.98 and from 1.09 to 1.29 with corresponding Reynolds numbers varying from about 0.94×10^6 to 1.27×10^6. From the results of this investigation it is concluded:

1. The trailing-edge flap was generally effective in producing an increment of lift at each angle of attack and Mach number. Small regions of ineffectiveness or of negative effectiveness, however, were evident at the highest subsonic Mach numbers for small flap deflections.

2. The variations with Mach number of the rate of change of flap-hinge-moment coefficient with flap deflection were relatively small except at Mach numbers near unity where comparatively large changes and reversals in sign occurred. The effect of Mach number on the rate of change of hinge-moment coefficient with angle of attack, however, was generally much greater than that on the rate of change of hinge-moment coefficient with flap deflection.

3. The effects of the flap-wing gaps at the lowest subsonic Mach numbers were to increase the drag coefficients and decrease the lift coefficients at the highest angles of attack. At the higher Mach numbers, the effects of the gaps were generally small.

Ames Aeronautical Laboratory,
    National Advisory Committee for Aeronautics,
        Moffett Field, Calif.

REFERENCES

1. Lange, Roy H. and May, Ralph W., Jr.: Effect of Leading-Edge High-Lift Devices and Split Flaps on the Maximum-Lift and Lateral Characteristics of a Rectangular Wing of Aspect Ratio 3.4 With Circular-Arc Airfoil Sections at Reynolds Numbers From 2.9×10^6 to 8.4×10^6. NACA RM L8D30, 1948.

2. Johnson, Ben H., Jr., and Bandettini, Angelo: Investigation of a Thin Wing of Aspect Ratio 4 in the Ames 12-Foot Pressure Wind Tunnel. II — The Effect of Constant-Chord Leading- and Trailing-Edge Flaps on the Low-Speed Characteristics of the Wing. NACA RM A8F15, 1948.

3. Johnson, Ben H., Jr., and Reed, Verlin D.: Investigation of a Thin
    Wing of Aspect Ratio 4 in the Ames 12—Foot Pressure Wind Tunnel.
    IV — The Effect of a Constant—Chord Leading—Edge Flap at High
    Subsonic Speeds. NACA RM A8K19, 1949.

4. Bandettini, Angelo, and Reed, Verlin D.: The Aerodynamic Charac-
    teristics Throughout the Subsonic Speed Range of a Thin, Sharp-
    Edged Horizontal Tail of Aspect Ratio 4 Equipped With a Constant—
    Chord Elevator. NACA RM A9E05, 1949.

5. Conner, D. William, and Mitchell, Meade H., Jr.: Control Effective-
    ness and Hinge—Moment Measurements at a Mach Number of 1.9 of a
    Nose Flap and Trailing—Edge Flap on a Highly Tapered Low—Aspect-
    Ratio Wing. NACA RM L8K17a, 1949.

6. Strass, H. Kurt: Free—Flight Investigation of the Rolling Effective-
    ness at High Subsonic, Transonic, and Supersonic Speeds of Leading—
    Edge and Trailing—Edge Ailerons in Conjunction With Tapered and
    Untapered Plan Forms. NACA RM L8E10, 1948.

7. Glauert, H.: Wind—Tunnel Interference on Wings, Bodies, and Air-
    screws. R & M No. 1566, British, A.R.C., 1933.

8. Goldstein, S., and Young, A. D.: The Linear Pertubation Theory of
    Compressible Flow With Applications to Wind—Tunnel Interference.
    R & M No. 1909, British, A.R.C., 1943.

9. Herriot, John G.: Blockage Corrections for Three—Dimensional—Flow
    Closed—Throat Wind Tunnels, With Consideration of the Effect of
    Compressibility. NACA RM A7B28, 1947.

10. DeYoung, John, and Harper, Charles W.: Theoretical Symmetric Span
    Loading at Subsonic Speeds for Wings Having Arbitrary Plan Form.
    NACA Rep. 921, 1948

11. Lagerstrom, Paco A., Wall, D., and Graham, M. E.: Formulas in
    Three—Dimensional Wing Theory (1). Douglas Aircraft Company
    Report No. SM—11901, August 1946.

12. Axelson, John A.: A Summary and Analysis of Wind—Tunnel Data on
    the Lift and Hinge—Moment Characteristics of Control Surfaces up
    to a Mach Number of 0.90. NACA RM A7L02, 1948.

TABLE I.— BASIC AERODYNAMIC DATA
$$[\delta_f = 10^\circ]$$

Gaps unsealed						Gaps sealed				
M	α	C_L	C_D	C_m	C_{h_f}	M	α	C_L	C_D	C_m
0.51	−3.0	−0.020	0.026	−0.014	−0.033	0.50	−3.0	−0.039	− − −	− − −
.72	−3.0	−.047	.030	−.021	−.022	.71	−3.0	−.044	− − −	− − −
.81	−3.0	−.087	.034	−.014	−.006	.82	−3.0	−.103	− − −	− − −
.88	−3.1	−.124	.039	−.005	.005	.87	−2.9	−.141	− − −	− − −
.91	−3.1	−.140	.043	.006	.014	.90	−2.9	−.183	− − −	− − −
.94	−3.1	−.160	.058	.024	.033	.92	−2.9	−.215	− − −	− − −
1.09	−3.0	−.072	.096	−.034	−.081	1.09	−3.0	−.055	0.074	− − −
1.20	−3.0	−.076	.080	−.044	−.109	1.20	−3.0	−.071	.078	−0.040
1.29	−3.0	−.041	.075	−.044	−.125	1.29	−3.0	−.041	.074	−.038
.51	.1	.104	.027	−.038	−.069	.51	.1	.167	.016	−.054
.72	.1	.096	.031	−.033	−.076	.71	.1	.115	.022	−.037
.81	0	.081	.033	−.026	−.072	.81	0	.088	.026	−.026
.88	0	.075	.036	−.025	−.072	.87	0	.064	.030	−.021
.91	0	.064	.040	−.021	−.066	.90	0	.067	.032	−.023
.94	0	.049	.047	−.014	−.059	.93	0	.019	.040	−.009
1.09	0	.098	.088	−.048	−.108	1.09	0	.096	.077	−.051
1.20	0	.076	.079	−.057	−.145	1.20	0	.093	.079	−.058
1.29	0	.096	.079	−.059	−.181	1.29	0	.107	.075	−.060
.51	3.1	.247	.037	−.033	−.118	.51	3.2	.330	.044	−.050
.72	3.1	.264	.042	−.023	−.146	.71	3.2	.284	.042	−.030
.81	3.1	.266	.046	−.020	−.153	.82	3.1	.272	.045	−.019
.88	3.2	.285	.053	−.023	−.164	.87	3.1	.278	.050	−.023
.90	3.2	.290	.055	−.026	−.170	.90	3.2	.287	.052	−.031
.94	3.1	.270	.062	−.031	−.177	.94	3.1	.250	.060	−.029
1.09	3.0	.272	.094	−.073	−.161	1.09	3.0	.286	.086	− − −
1.20	3.0	.226	.087	−.071	−.176	1.20	3.0	.256	.081	− − −
1.29	3.0	.246	.081	−.072	−.200	1.29	3.0	.253	.084	−.070
.51	6.2	.406	.061	−.045	−.131	.51	6.2	.456	.061	−.128
.72	6.2	.449	.069	−.023	−.127	.72	6.2	.459	.067	−.056
.81	6.2	.464	.074	−.029	−.131	.82	6.2	.454	.068	−.046
.88	6.3	.504	.081	−.035	−.129	.87	6.3	.484	.076	−.045
.91	6.3	.515	.090	−.049	−.142	.91	6.3	.482	.075	−.052
.95	6.3	.517	.114	−.083	−.184	.95	6.2	.469	.111	−.067
1.09	6.0	.469	.115	− − −	−.194	.97	6.2	.469	.129	−.085
1.20	6.0	.399	.112	−.092	−.213	1.09	6.0	.477	.114	−.092
1.29	6.0	.400	.106	−.091	−.240	1.20	6.0	.405	.091	− − −
						1.29	6.0	.416	.113	−.085
.52	9.2	.472	.123	−.070	−.156					
.72	9.3	.500	.122	−.070	−.156	.51	9.3	.561	.115	−.102
.82	9.3	.525	.123	−.050	−.165	.72	9.3	.598	.127	−.058
.88	9.3	.620	.132	−.034	−.180	.82	9.3	.634	.131	−.044
.91	9.3	.651	.145	−.052	−.205	.88	9.3	.620	.140	−.054
.94	9.4	.702	.171	−.075	−.254	1.20	9.0	.585	.148	− − −
.96	9.4	.721	.196	−.097	−.323	1.29	9.0	.574	.160	−.095
1.20	9.0	.563	.153	−.107	−.260					
1.29	9.0	.547	.151	−.107	−.282	.51	12.4	.747	.192	−.036
						.71	12.4	.750	.205	−.033
.51	12.3	.495	.200	−.066	−.274	.82	12.4	.750	.215	−.043
.72	12.3	.524	.204	−.059	−.297	.88	12.4	.788	.223	−.044
.82	12.3	.579	.213	−.058	−.310	.90	12.4	.835	.238	−.050
.89	12.3	.615	.221	−.077	−.336	1.20	12.0	.772	.208	− − −
.92	12.4	.716	.259	−.105	−.398	1.29	12.0	.718	.223	− − −
1.20	12.0	.723	.211	−.125	−.291					
1.29	12.0	.663	.209	− − −	−.323					

NACA

TABLE II.— BASIC AERODYNAMIC DATA
$[\delta_f = 20°]$

Gaps unsealed					
M	α	c_L	c_D	c_m	c_{h_f}
0.51	−2.9	0.080	0.043	−0.060	−0.109
.72	−3.0	.060	.047	−.066	−.115
.82	−3.0	.044	.051	−.066	−.118
.88	−3.0	.025	.056	−.064	−.118
.91	−3.0	.022	.063	−.063	−.129
.94	−3.0	.023	.067	−.064	−.140
1.09	−3.0	.024	.107	−.096	−.252
1.20	−3.0	.038	.102	−.100	−.279
1.29	−3.0	.047	.101	−.101	−.295
.51	.1	.203	.054	−.072	−.153
.72	.1	.213	.059	−.074	−.194
.82	.1	.222	.065	−.079	−.217
.88	.1	.216	.069	−.075	−.233
.91	.1	.239	.078	−.093	−.264
.94	.1	.254	.095	−.104	−.315
1.09	0	.255	.113	−.126	−.299
1.20	0	.191	.112	−.112	−.361
1.29	0	.209	.109	−.127	−.382
.51	3.2	.368	.074	−.070	−.235
.72	3.2	.392	.082	−.071	−.297
.82	3.2	.405	.087	−.076	−.316
.88	3.2	.435	.096	−.085	−.337
.91	3.2	.460	.105	−.099	−.354
.95	3.3	.492	.135	−.126	−.417
1.09	3.0	.467	.142	−.141	−.328
1.20	3.0	.368	.128	−.146	−.402
1.29	3.0	.364	.129	−.146	−.427
.51	6.3	.541	.135	−.129	−.304
.72	6.3	.600	.140	−.115	−.335
.83	6.3	.653	.145	−.101	−.353
.88	6.4	.704	.159	−.134	−.368
.92	6.4	.723	.180	−.158	−.405
.95	6.4	.734	.209	−.176	−.469
1.20	6.0	.545	.161	− − −	−.421
1.29	6.0	.537	.168	−.165	−.476
.51	9.3	.616	.207	−.142	−.349
.73	9.3	.681	.221	−.129	−.364
.81	9.4	.726	.226	−.136	−.196
.88	9.4	.796	.235	−.153	−.404
.93	9.5	.911	.275	−.184	−.473
.94	9.5	.942	.311	−.208	−.512
1.20	9.0	.749	.215	−.183	−.446
1.29	9.0	.680	.222	−.178	−.492
.53	12.3	.664	.281	−.099	−.411
.72	12.4	.677	.281	−.102	−.390
.82	12.4	.729	.291	−.121	−.413
.88	12.4	.769	.302	−.132	−.438
.92	12.5	.893	.352	−.161	− − −
.94	12.5	1.006	.415	−.190	− − −
1.20	12.0	.873	.275	− − −	−.453
1.29	12.0	.812	.292	− − −	−.525

NACA
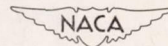
TABLE III.— BASIC AERODYNAMIC DATA

$[\delta_f = 40°]$

Gaps unsealed					
M	α	c_L	c_D	c_m	c_{h_f}
0.51	−2.8	0.331	0.111	−0.160	−0.266
.72	−2.8	.310	.124	−.154	−.289
.82	−2.8	.306	.135	−.162	−.317
.88	−2.9	.303	.147	−.165	−.341
.92	−2.9	.301	.164	−.170	−.368
.51	.3	.497	.143	−.156	−.311
.72	.3	.497	.161	−.156	−.344
.82	.3	.497	.169	−.165	−.368
.88	.3	.498	.181	−.172	−.396
.92	.3	.509	.207	−.189	−.437
.51	3.3	.647	.191	−.172	−.356
.72	3.3	.664	.215	−.164	−.385
.83	3.4	.685	.228	−.172	−.412
.89	3.4	.722	.255	−.195	−.463
.93	3.4	.736	.298	−.216	−.519
.51	6.4	.796	.266	−.175	−.406
.72	6.4	.820	.279	−.172	−.422
.83	6.5	.885	.298	−.201	−.475
.89	6.5	.910	.314	−.205	−.531
.93	6.5	.926	.396	−.248	−.634
.51	9.5	.888	.343	−.181	−.444
.72	9.5	.906	.349	−.196	−.461
.82	9.5	.946	.368	−.216	−.504
.89	9.5	.981	.392	−.227	−.550
.51	12.5	.892	.416	−.168	−.452
.72	12.5	.917	.421	−.200	−.480
.83	12.5	1.033	.459	−.224	−.541
.90	12.5	1.108	.527	−.256	−.641

NACA

TABLE IV.— BASIC AERODYNAMIC DATA
[$\delta_f = 60°$]

Gaps unsealed

M	α	C_L	C_D	C_m	C_{h_f}
0.51	−2.7	0.502	0.196	−0.171	−0.392
.72	−2.8	.495	.216	−.176	−.416
.82	−2.8	.490	.243	−.181	−.444
.89	−2.8	.478	.266	−.180	−.474
.51	.3	.650	.228	−.191	−.430
.72	.3	.651	.252	−.188	−.449
.82	.3	.656	.274	−.186	−.478
.51	3.4	.796	.273	−.202	−.472
.72	3.4	.839	.308	−.199	−.498
.82	3.4	.833	.325	−.208	−.520
.89	3.4	.839	.359	−.229	−.569
.51	6.5	.933	.361	−.204	−.502
.72	6.5	.960	.387	−.220	−.529
.82	6.5	.989	.404	−.229	−.562
.89	6.5	.985	.444	−.252	−.616
.51	9.5	1.008	.434	−.181	−.520
.72	9.5	1.049	.460	−.196	−.556
.83	9.5	1.064	.484	−.212	−.594
.90	9.6	1.134	.634	−.285	−.751
.51	12.5	1.039	.530	−.194	−.555
.72	12.5	1.031	.545	−.208	−.576
.83	12.5	1.016	.580	−.225	−.624

Gaps sealed

M	α	C_L	C_D	C_m
0.51	−2.7	0.571	0.202	−0.159
.72	−2.7	.578	.213	−.179
.82	−2.7	.580	.237	−.185
.88	−2.7	.574	.263	−.195
.51	.4	.670	.225	−.162
.72	.4	.732	.243	−.177
.82	.4	.750	.272	−.187
.88	.4	.752	.291	−.208
.51	3.4	.842	.265	−.154
.72	3.5	.893	.291	−.156
.82	3.5	.925	.322	−.186
.89	3.5	.952	.341	−.218
.51	6.5	1.022	.344	−.173
.72	6.6	1.129	.378	−.215
.82	6.6	1.163	.404	−.225
.89	6.6	1.185	.436	−.249
.91	6.6	1.155	.555	−.312
.51	9.6	1.168	.443	−.215
.72	9.6	1.195	.478	−.231
.82	9.7	1.279	.508	−.224
.89	9.7	1.324	.595	−.301
.90	9.7	1.320	.662	−.323
.51	12.6	1.166	.552	−.170
.73	12.6	1.118	.560	− − −
.82	12.6	1.155	.599	−.200

TABLE V.— BASIC AERODYNAMIC DATA
$$[\delta_f = -10°]$$

Gaps unsealed

M	α	c_L	c_D	c_m	c_{h_f}
0.51	−3.1	−0.254	0.044	0.031	0.056
.72	−3.1	−.257	.045	.024	.056
.82	−3.1	−.271	.047	.018	.055
.86	−3.2	−.286	.050	.022	.052
.91	−3.2	−.295	.053	.029	.050
.93	−3.1	−.283	.061	.034	.067
.98	−3.2	−.305	.098	.069	.180
1.09	−3.0	−.273	.094	.089	.184
1.20	−3.0	−.265	.084	.076	.162
1.29	−3.0	−.242	.086	.062	.188
.51	−.1	−.106	.029	.044	.059
.72	−.1	−.091	.031	.047	.057
.81	0	−.083	.034	.038	.046
.86	0	−.086	.039	.048	.046
.91	0	−.073	.042	.045	.036
.94	0	−.053	.047	.036	.031
.98	−.1	−.092	.082	.043	.092
1.09	0	−.079	.086	.050	.135
1.20	0	−.118	.077	.064	.136
1.29	0	−.092	.074	.056	.165
.51	3.0	.029	.022	.024	.065
.72	3.0	.069	.028	.026	.068
.81	3.0	.096	.032	.023	.064
.86	3.1	.125	.040	.026	.064
.91	3.1	.150	.044	.011	.057
.96	3.1	.120	.074	.007	.059
1.09	3.0	.089	.086	– – –	.086
1.20	3.0	.038	.074	.036	.114
1.29	3.0	.055	.073	.036	.136
.51	6.1	.175	.034	.017	.045
.72	6.1	.233	.042	.028	.044
.82	6.2	.287	.052	.029	.037
.88	6.2	.327	.062	.031	.035
.92	6.2	.362	.070	−.002	.018
.97	6.2	.320	.116	.014	.032
.98	6.2	.293	.114	.014	.065
1.09	6.0	.280	.091	.019	.082
1.20	6.0	.208	.088	.025	.092
1.29	6.0	.219	.089	.025	.098
.51	9.1	.245	.075	.028	.095
.72	9.2	.330	.086	.035	.076
.82	9.2	.408	.097	.018	.053
.88	9.3	.501	.103	.013	.023
.91	9.3	.560	.125	−.005	.009
.95	9.3	.521	.167	.010	.064
1.20	9.0	.379	.121	−.003	.069
1.29	9.0	.364	.121	.003	.069
.51	12.1	.236	.117	.039	.060
.72	12.2	.316	.137	.024	.054
.82	12.2	.387	.150	.018	.033
.89	12.2	.419	.167	.026	.042
.92	12.2	.457	.189	.035	.079
1.20	12.0	.517	.170	– – –	.065
1.29	12.0	.505	.170	−.015	.050

Gaps sealed

M	α	c_L	c_D	c_m
0.51	−3.2	−0.332	0.045	0.059
.72	−3.2	−.310	.039	.055
.82	−3.2	−.306	.044	.054
.88	−3.2	−.335	.049	.067
.91	−3.2	−.336	.053	.091
.94	−3.2	−.314	.067	.088
1.09	−3.0	−.297	.083	.086
1.20	−3.0	−.270	.084	.082
1.29	−3.0	−.239	.086	.076
.51	−.1	−.186	.032	.053
.72	−.1	−.144	.032	.044
.82	−.1	−.125	.034	.042
.88	−.1	−.121	.038	.045
.91	−.1	−.116	.039	.046
.94	0	−.086	.051	.041
1.09	0	−.096	.074	.057
1.20	0	−.120	.074	.060
1.29	0	−.088	.075	.068
.51	3.0	−.041	.019	.048
.72	3.0	.024	.027	.041
.82	3.0	.063	.033	.036
.88	3.1	.096	.039	.029
.91	3.1	.146	.038	.010
.94	3.1	.162	.057	−.002
1.09	3.0	.101	.076	.029
1.20	3.0	.049	.073	.038
.51	6.0	.106	.027	.056
.72	6.1	.201	.041	.053
.82	6.1	.252	.052	.045
.88	6.1	.311	.065	.035
.91	6.2	.368	.077	.009
.95	6.2	.367	.099	−.001
1.09	6.0	.294	.095	.018
1.20	6.0	.233	.091	.028
1.29	6.0	.237	.088	.031
.51	9.1	.249	.050	.066
.72	9.2	.386	.079	.050
.82	9.2	.468	.093	.049
.88	9.3	.541	.113	.002
.92	9.3	.602	.140	−.030
.95	9.3	.535	.176	−.009
1.20	9.0	.418	.128	−.001
1.29	9.0	.395	.128	.004
.51	12.2	.367	.097	.062
.72	12.3	.515	.142	.024
.82	12.3	.565	.159	−.006
.88	12.3	.630	.173	−.005
.92	12.4	.690	.212	−.023
1.20	12.0	.581	.178	−.016
1.29	12.0	.549	.180	−.013

NACA

Figure 1.— Illustration of the flexible—throat mechanism in the Ames 1—by $3\frac{1}{2}$—foot high-speed wind tunnel.
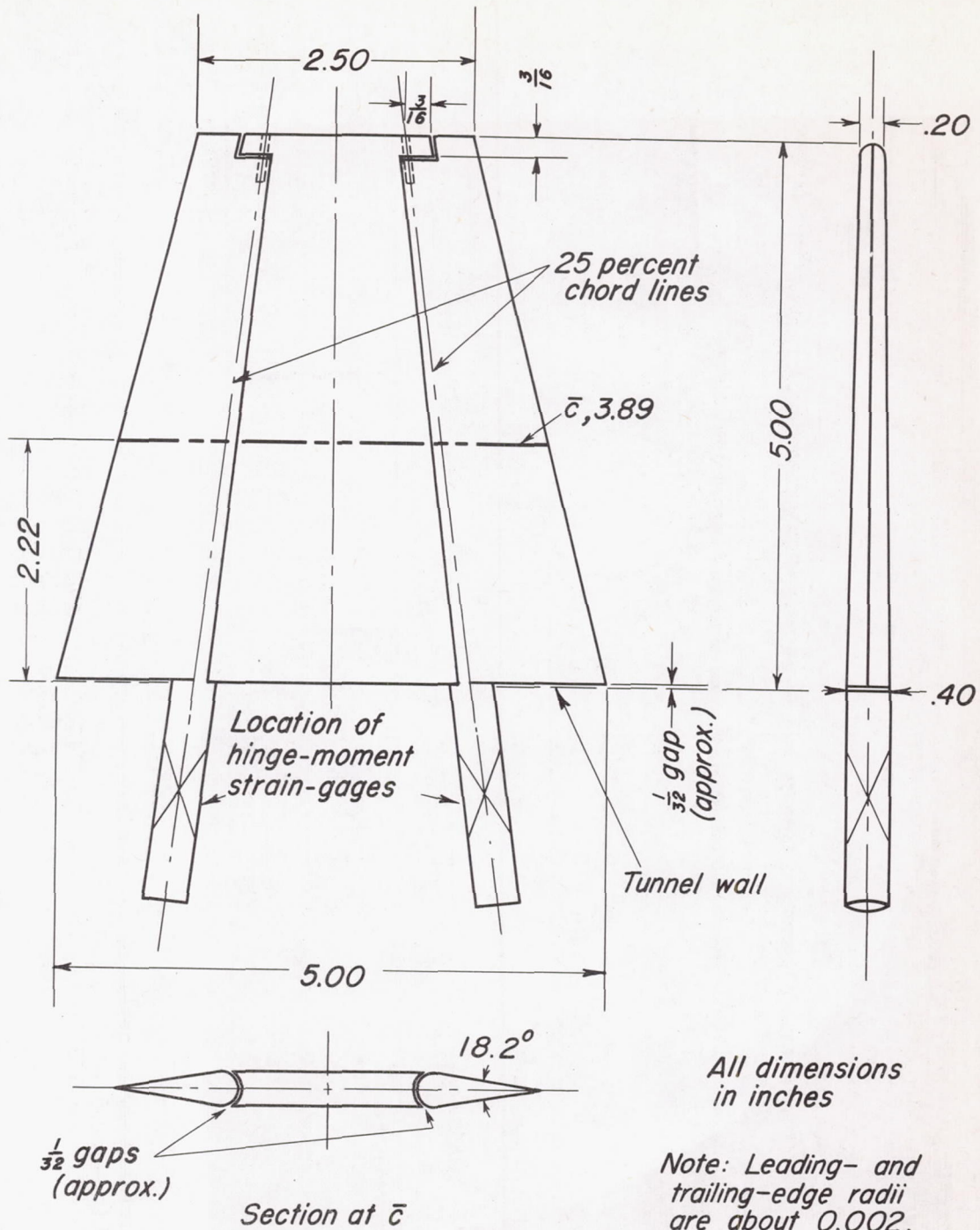
Figure 2.— Sketch of the semispan wing model with leading- and trailing-edge flaps.
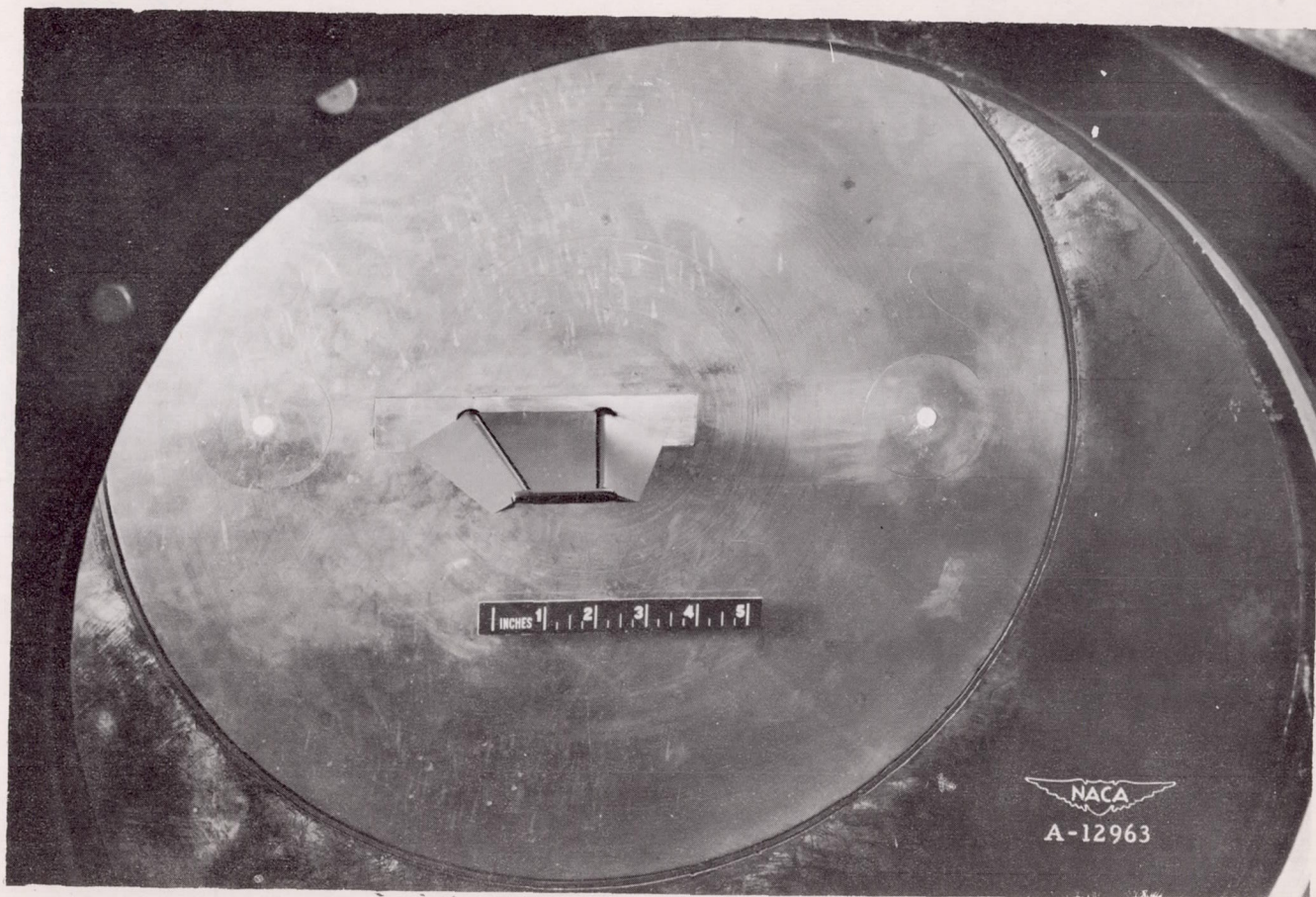
Figure 3.— Photograph of the model with the leading— and trailing—edge flaps
deflected, mounted on the semispan balance in the Ames 1— by 3—1/2—foot
high—speed wind tunnel.
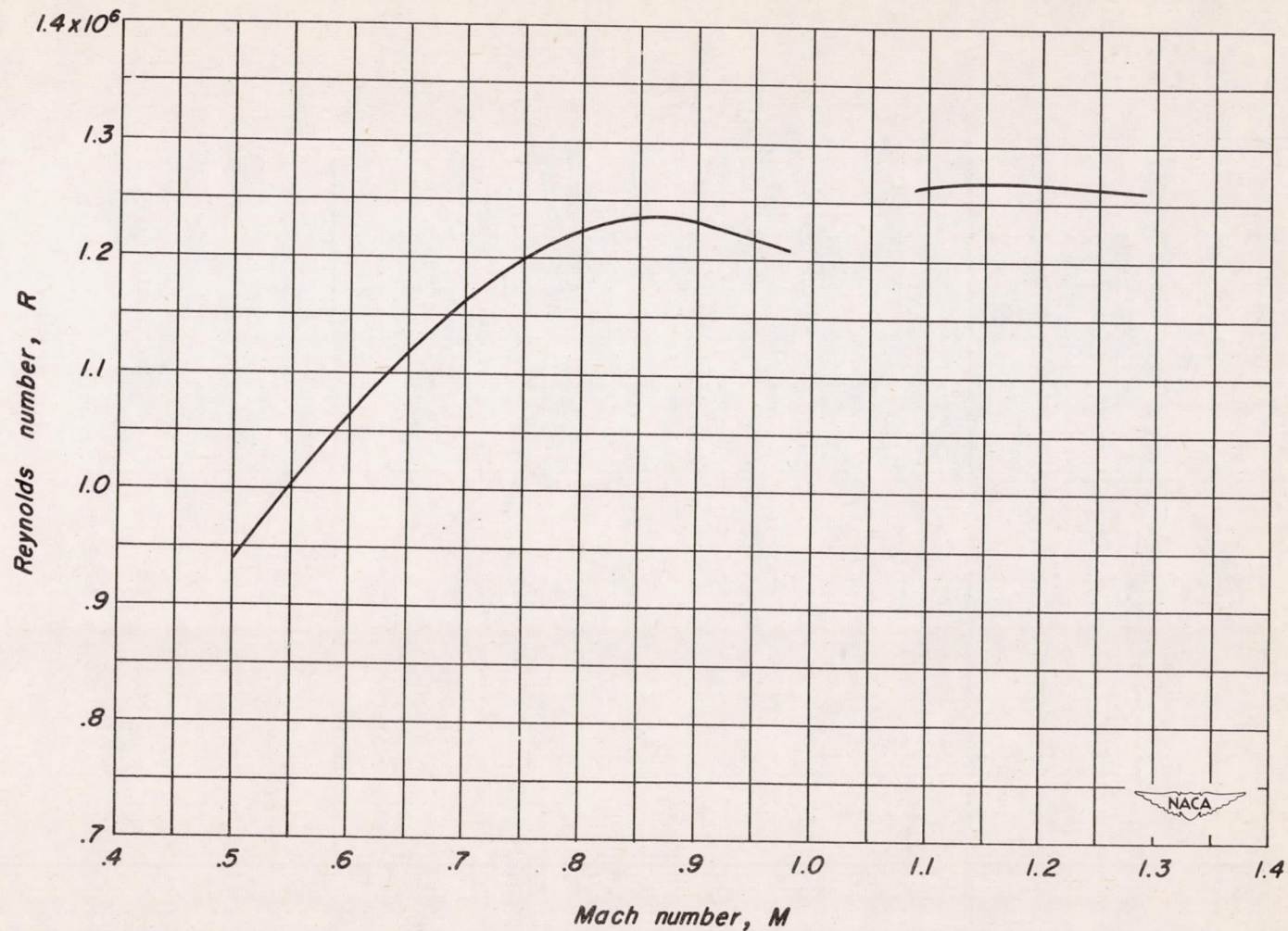
Figure 4.— Nominal variation of Reynolds number with Mach number for tests of the semispan wing of aspect ratio 2.67 in the Ames 1- by $3\frac{1}{2}$-foot high-speed wind tunnel.
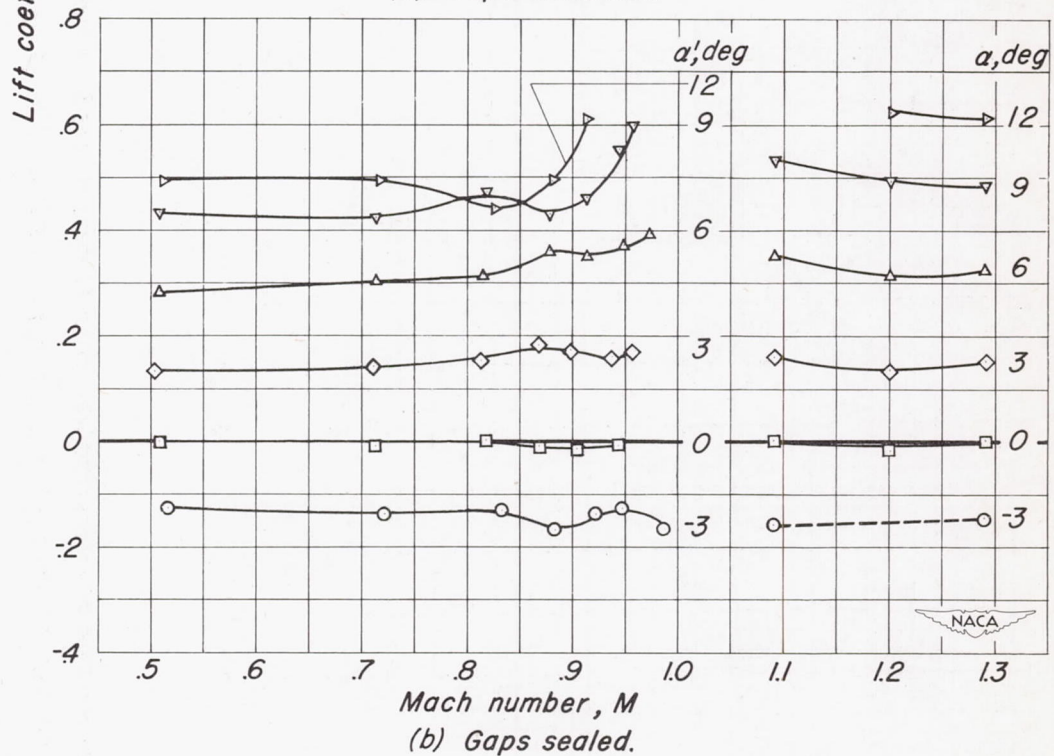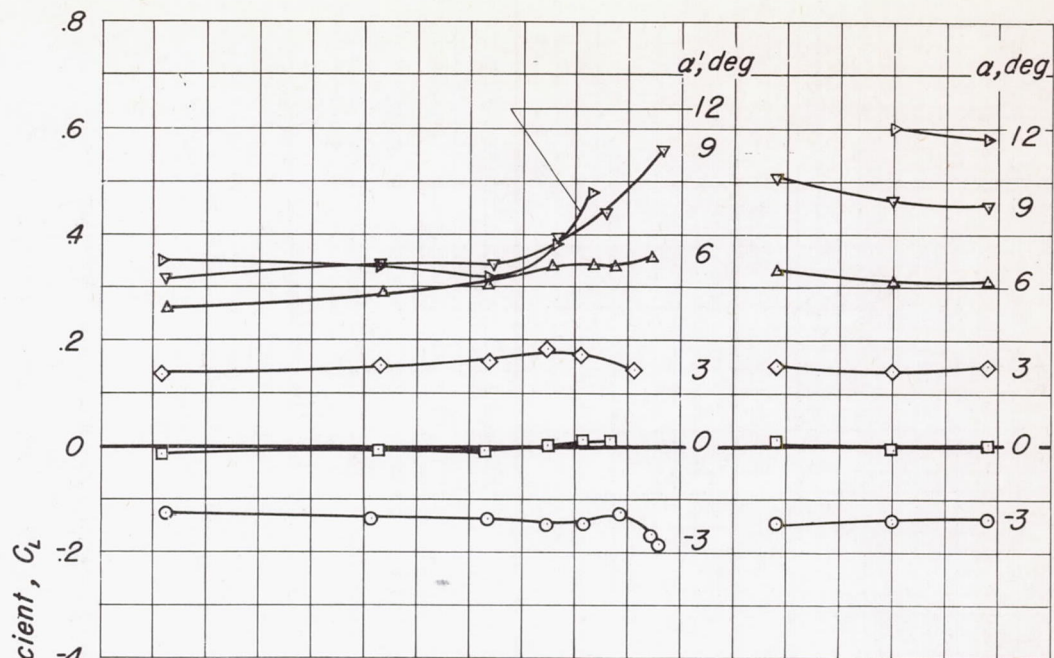
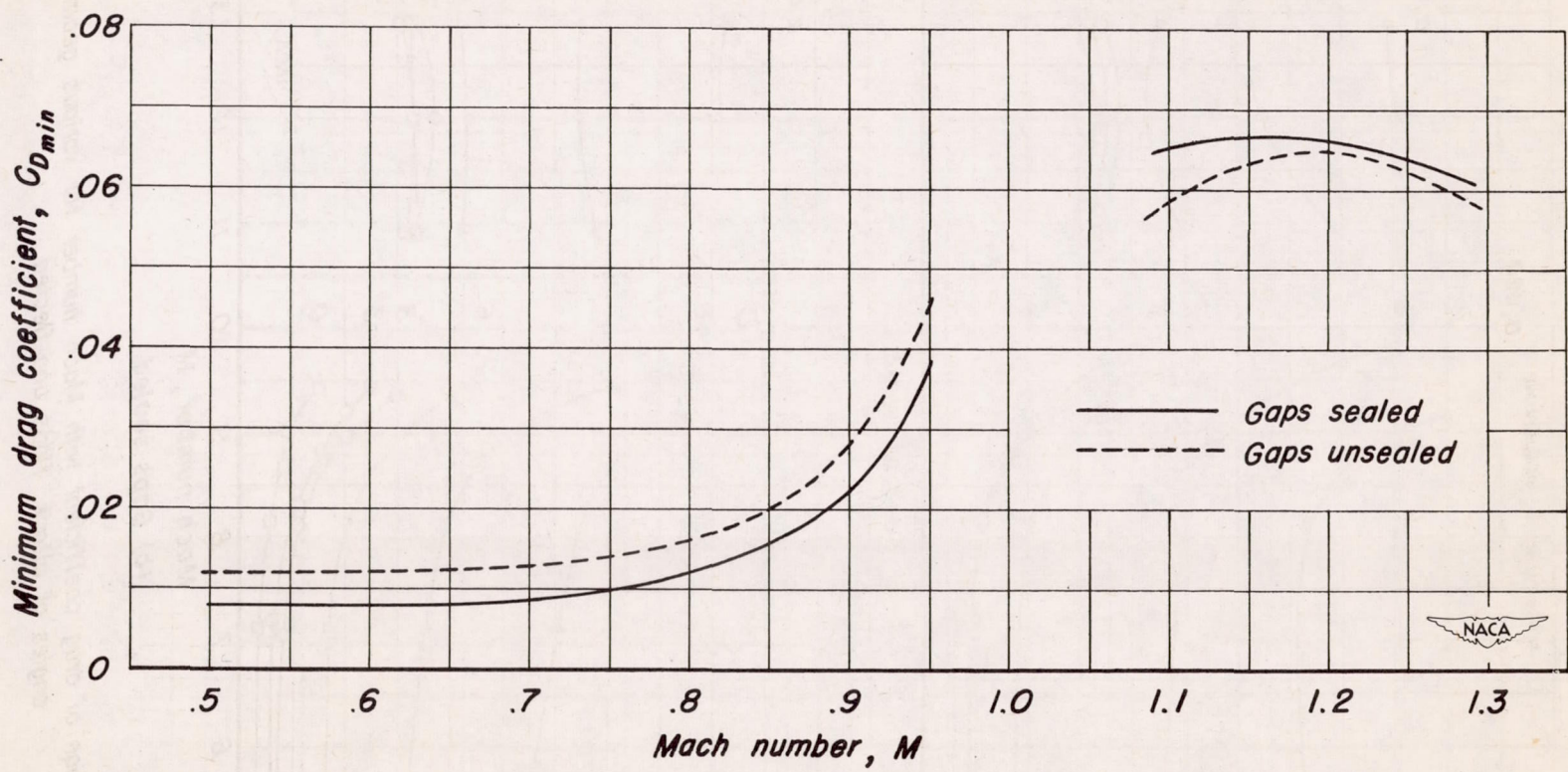Figure 5.— Variation of lift coefficient with Mach number for various geometric angles of attack, flaps undeflected.
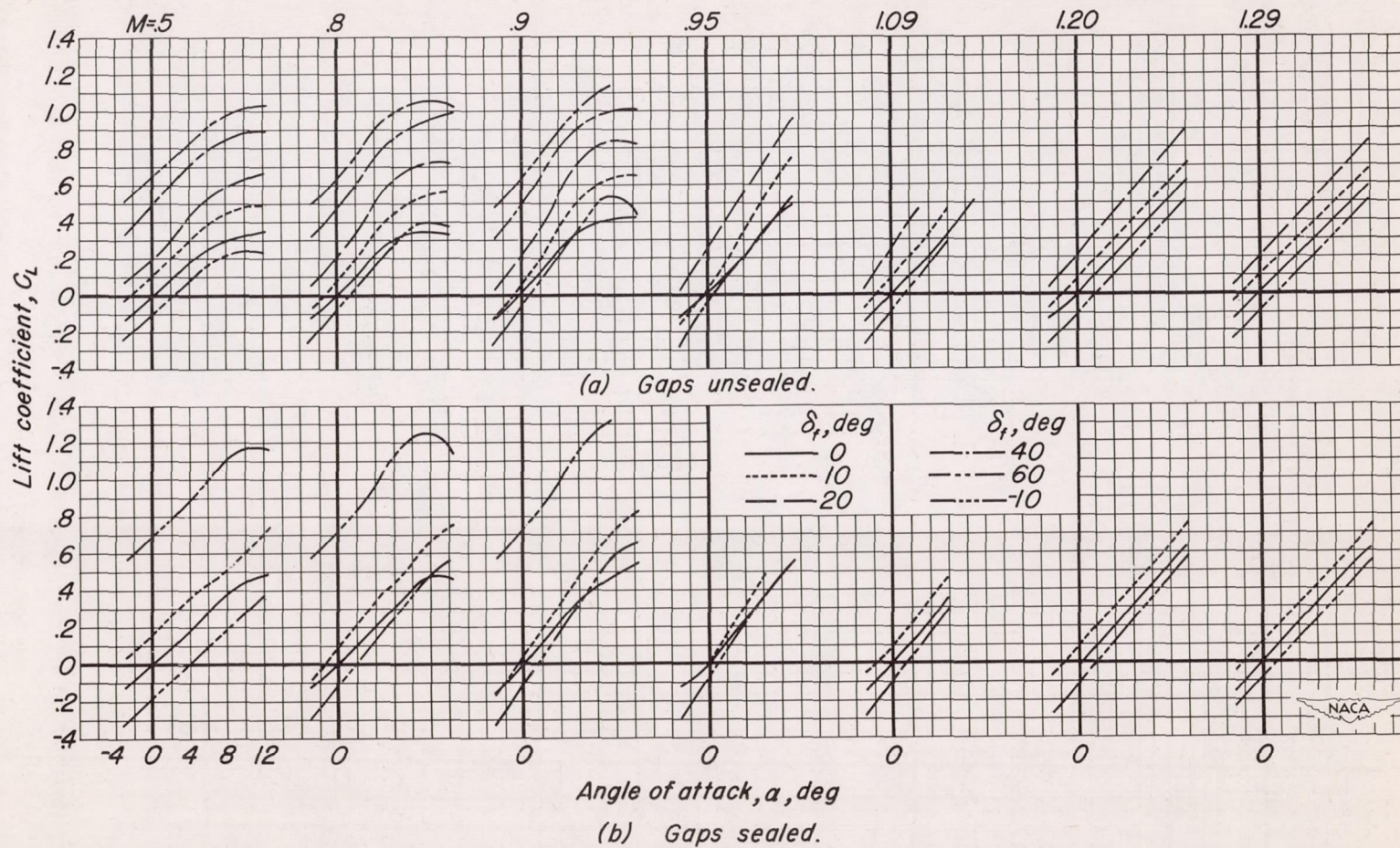
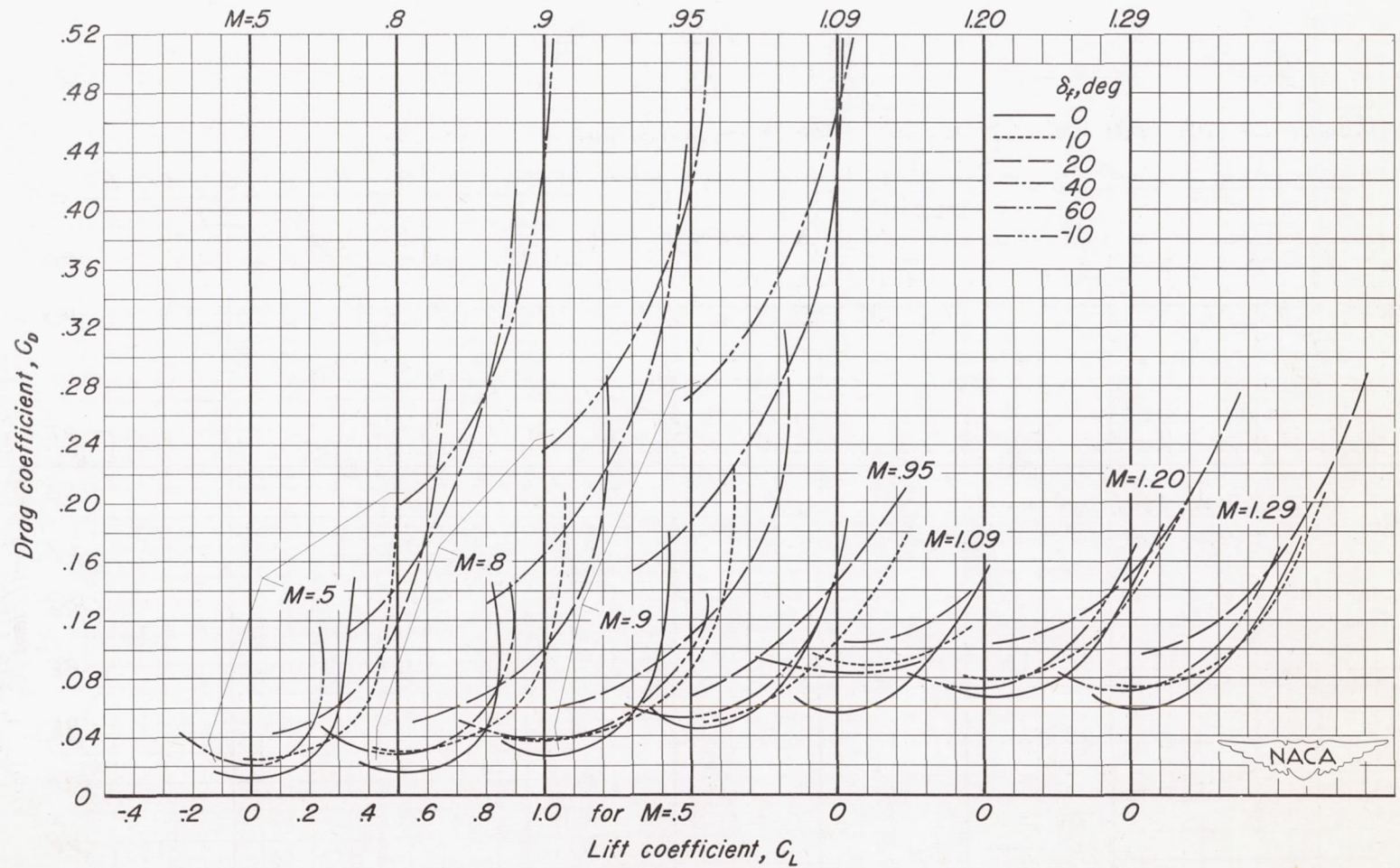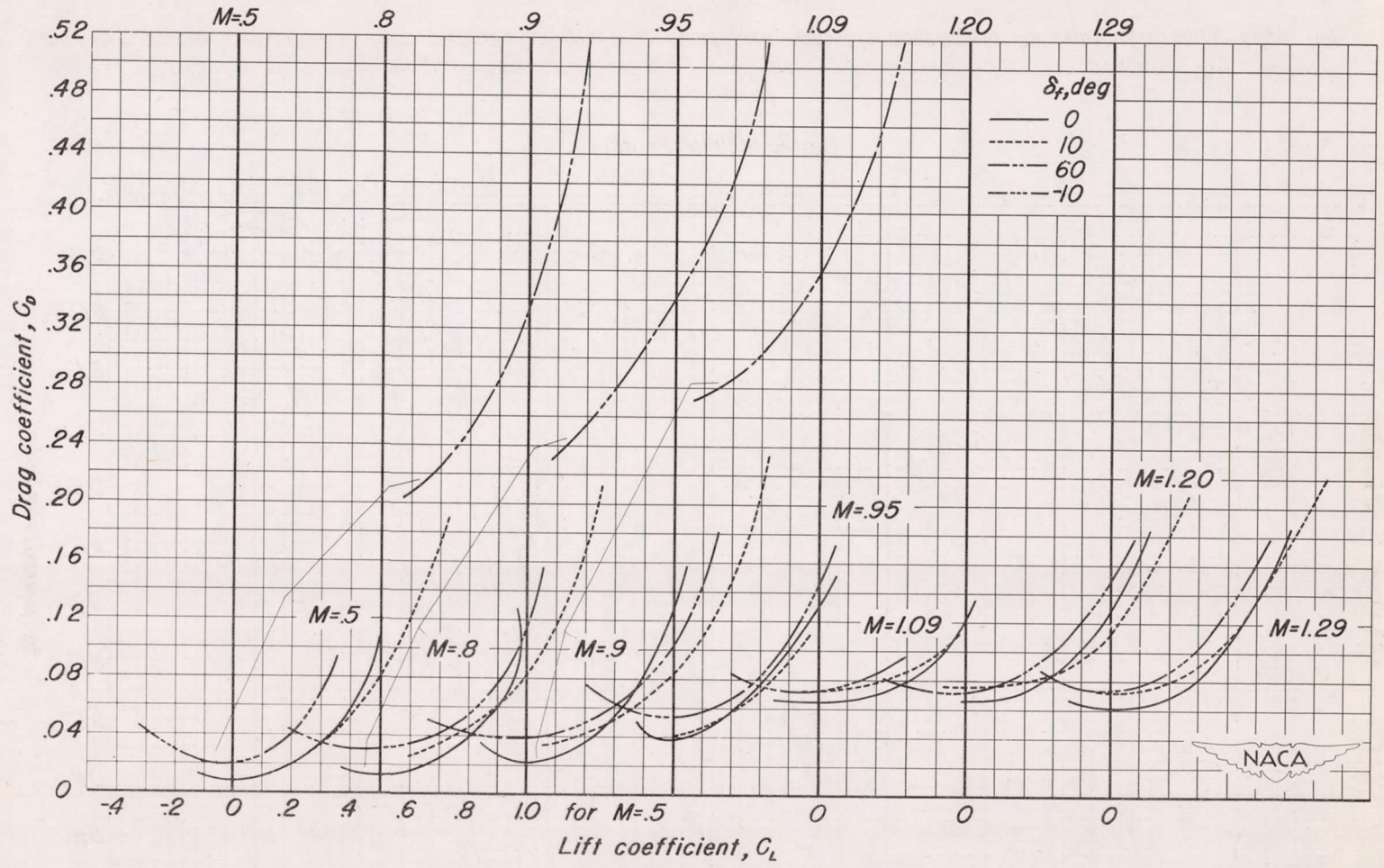Figure 6.– Variation at several Mach numbers of lift coefficient with angle of attack for various trailing–edge flap deflections.
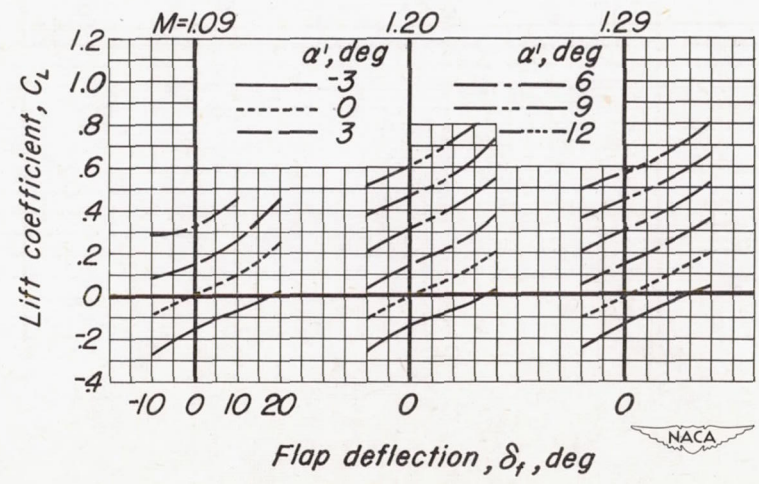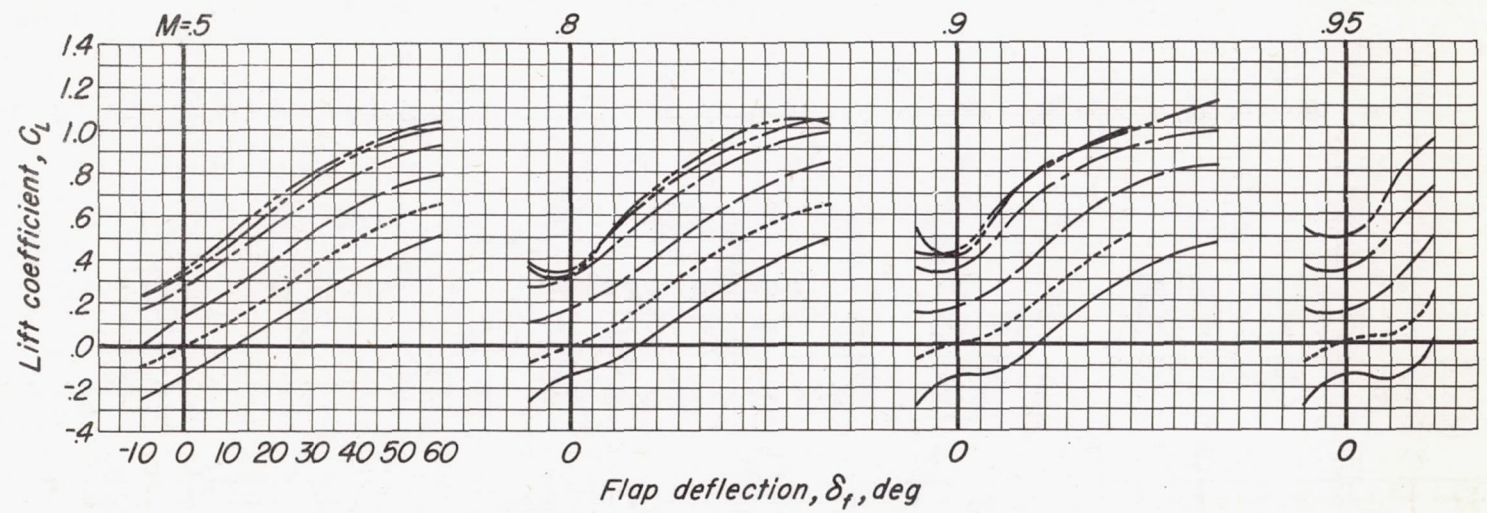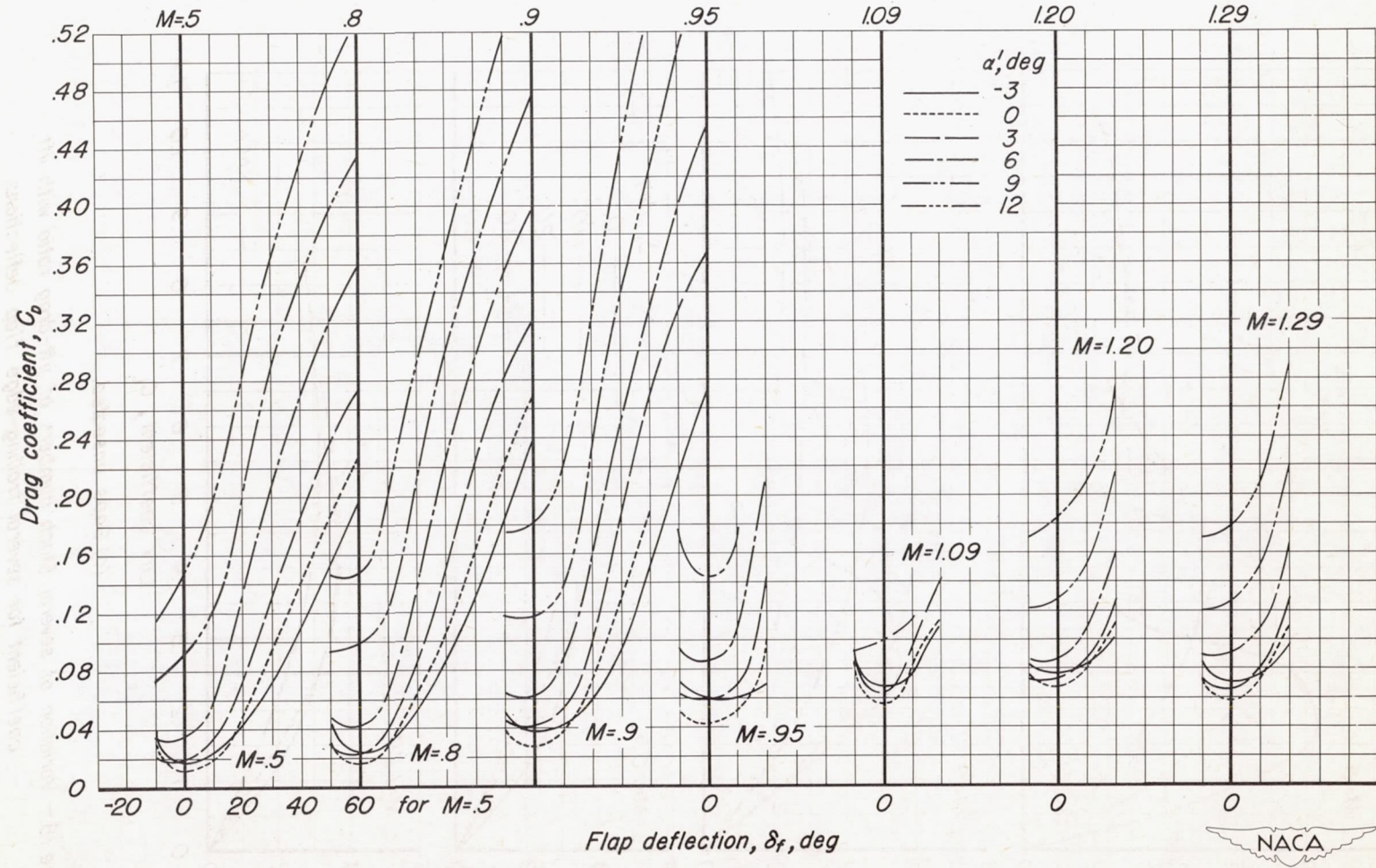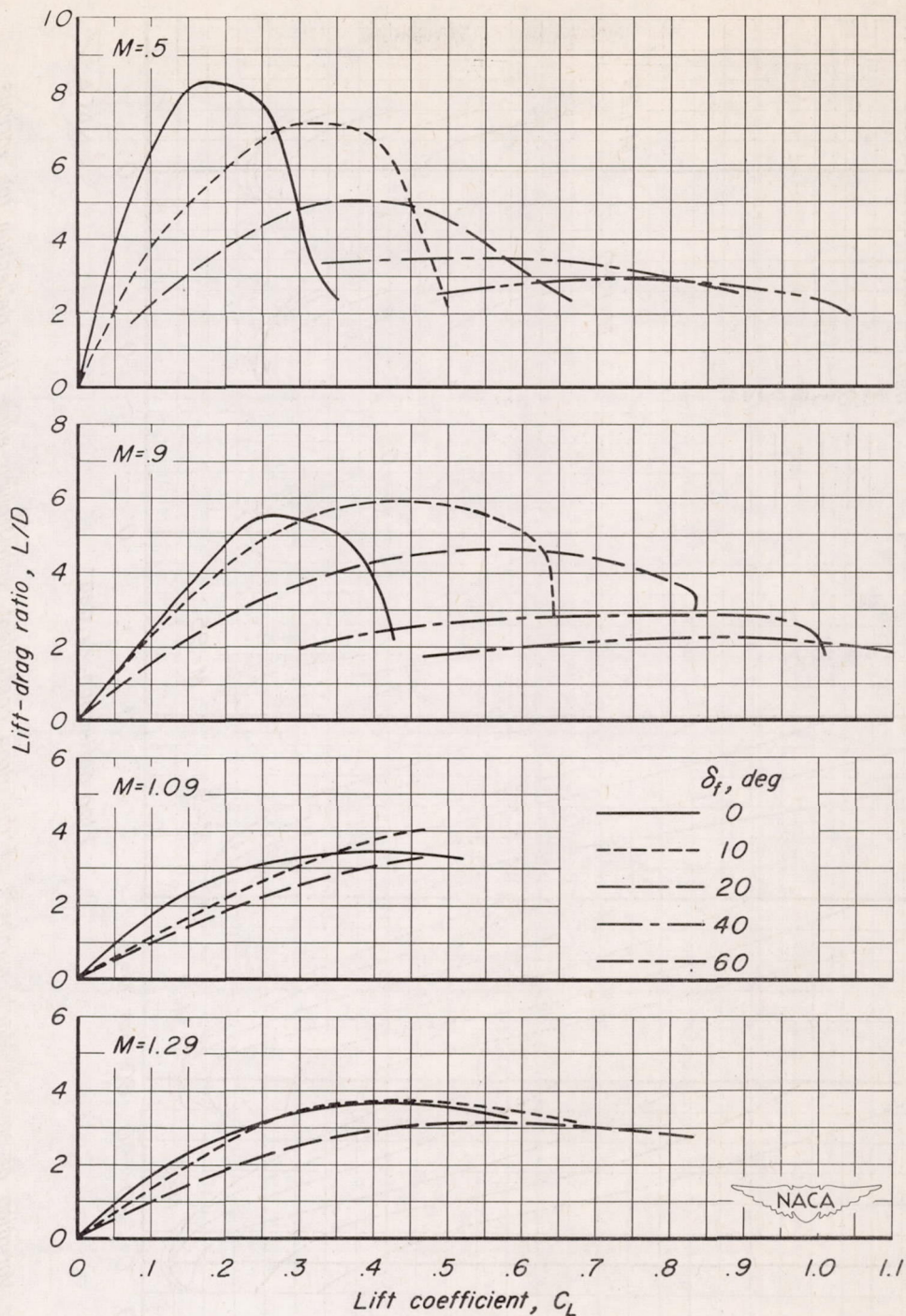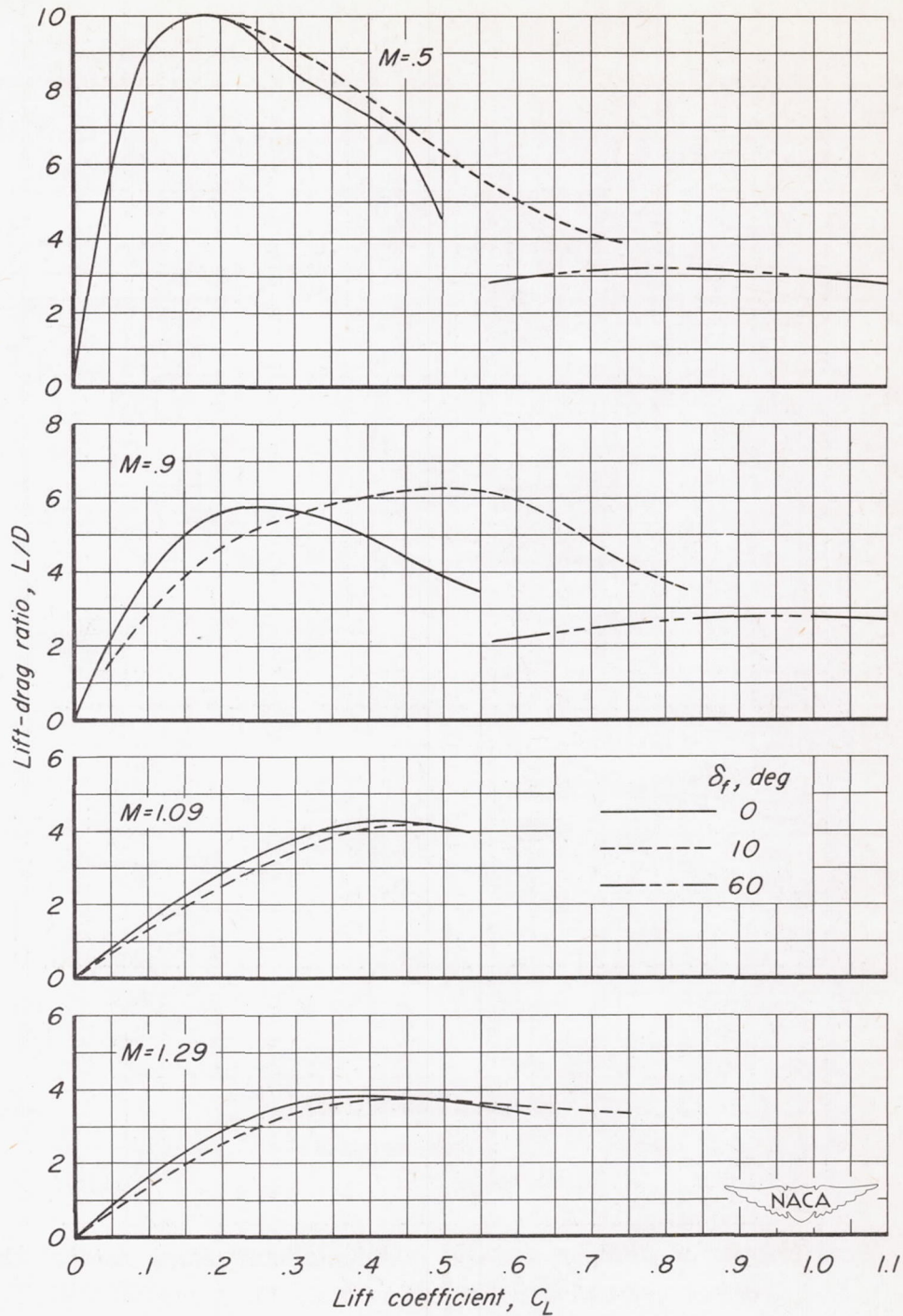
(a) Gaps unsealed.

Figure 7.— Variation at several Mach numbers of lift coefficient with trailing—edge flap deflection for various geometric angles of attack.
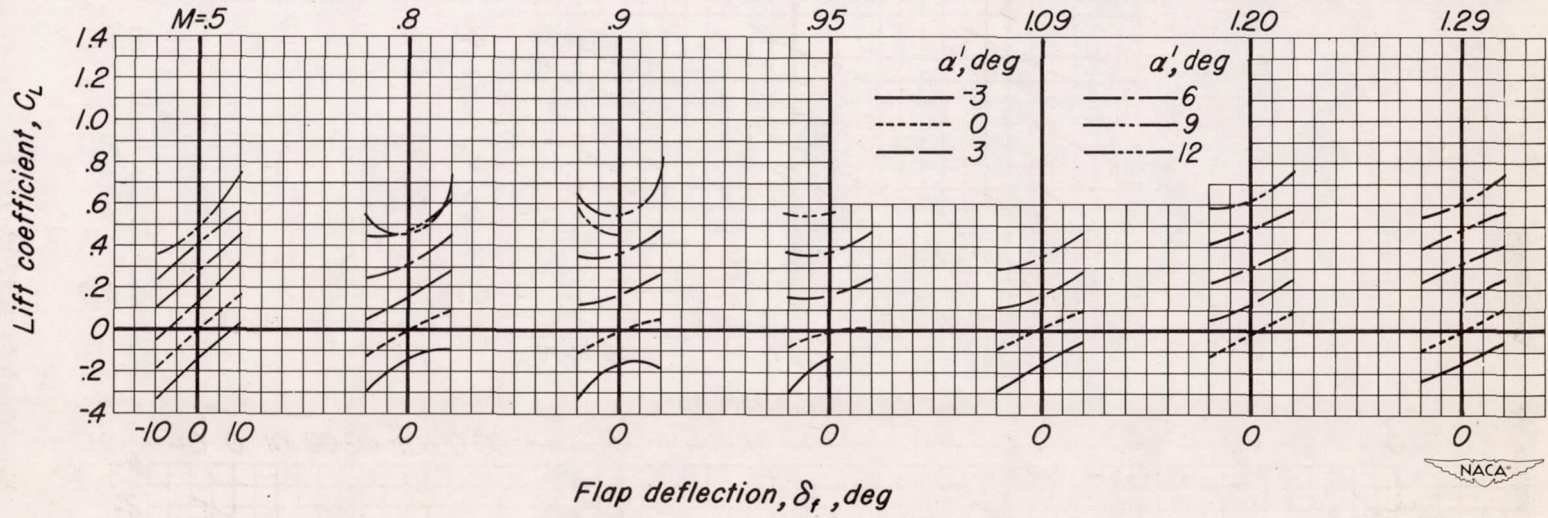
(b) Gaps sealed.

Figure 7.— Concluded.
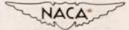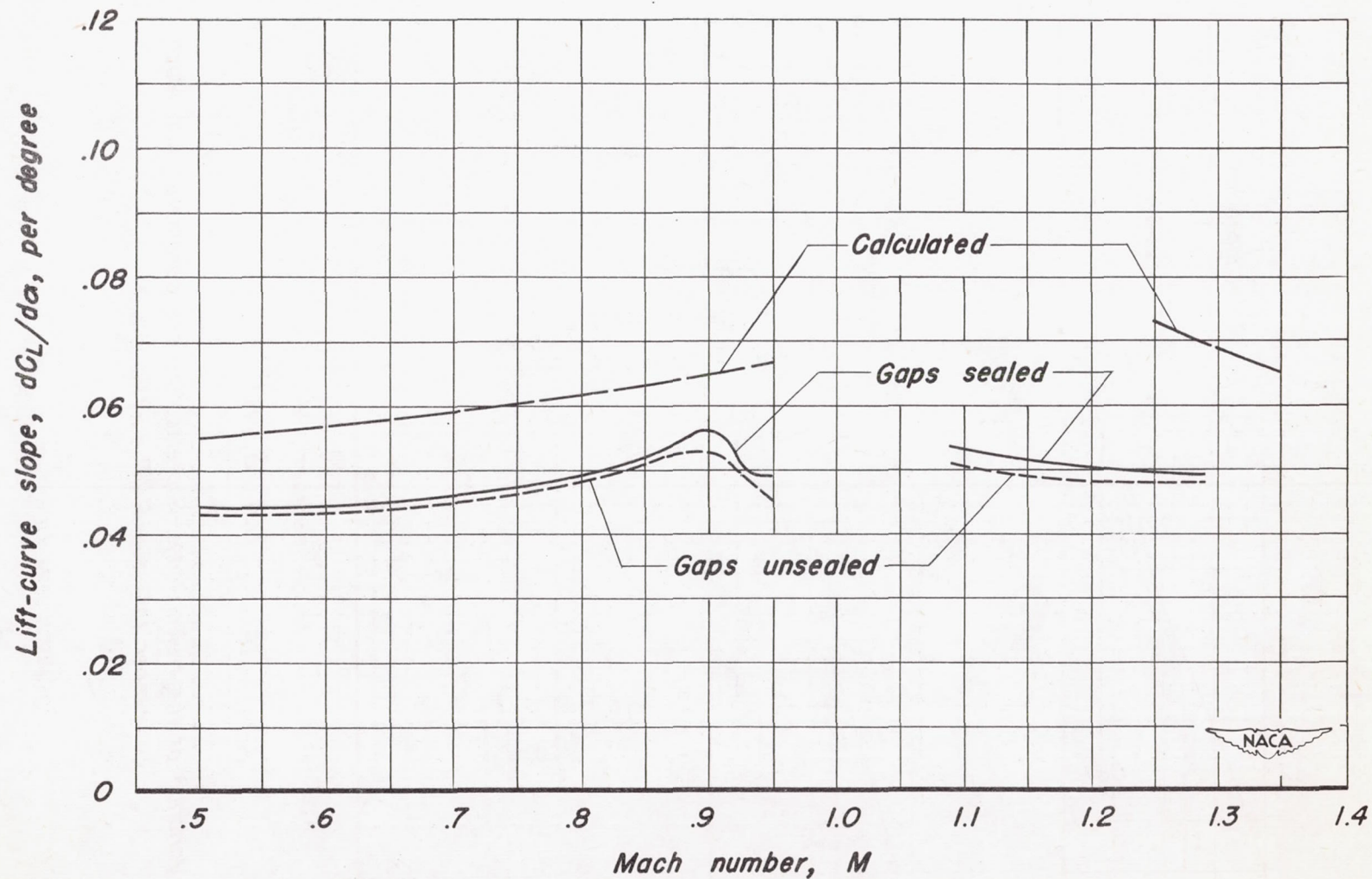
Figure 8.— Effect of Mach number on the lift-curve slopes near zero angle of attack for the wing with undeflected flaps.

(a) C_L, 0; δ_f, 0.

(b) C_L, 0.2; δ_f, 0.

(c) C_L, 0.4; δ_f, $10°$.
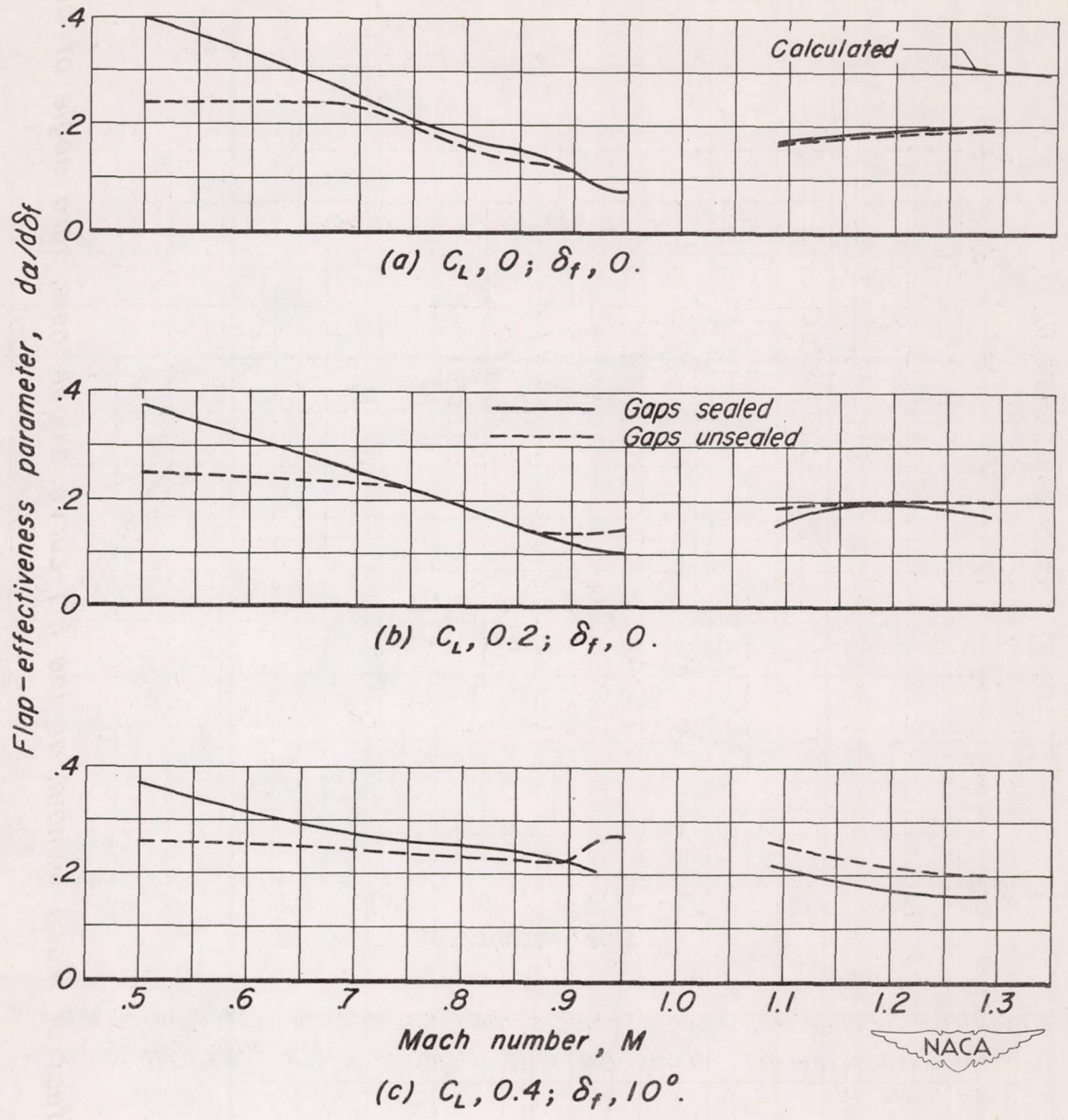
Figure 9.— Variation of the trailing-edge-flap effectiveness parameter with Mach number for several lift coefficients.
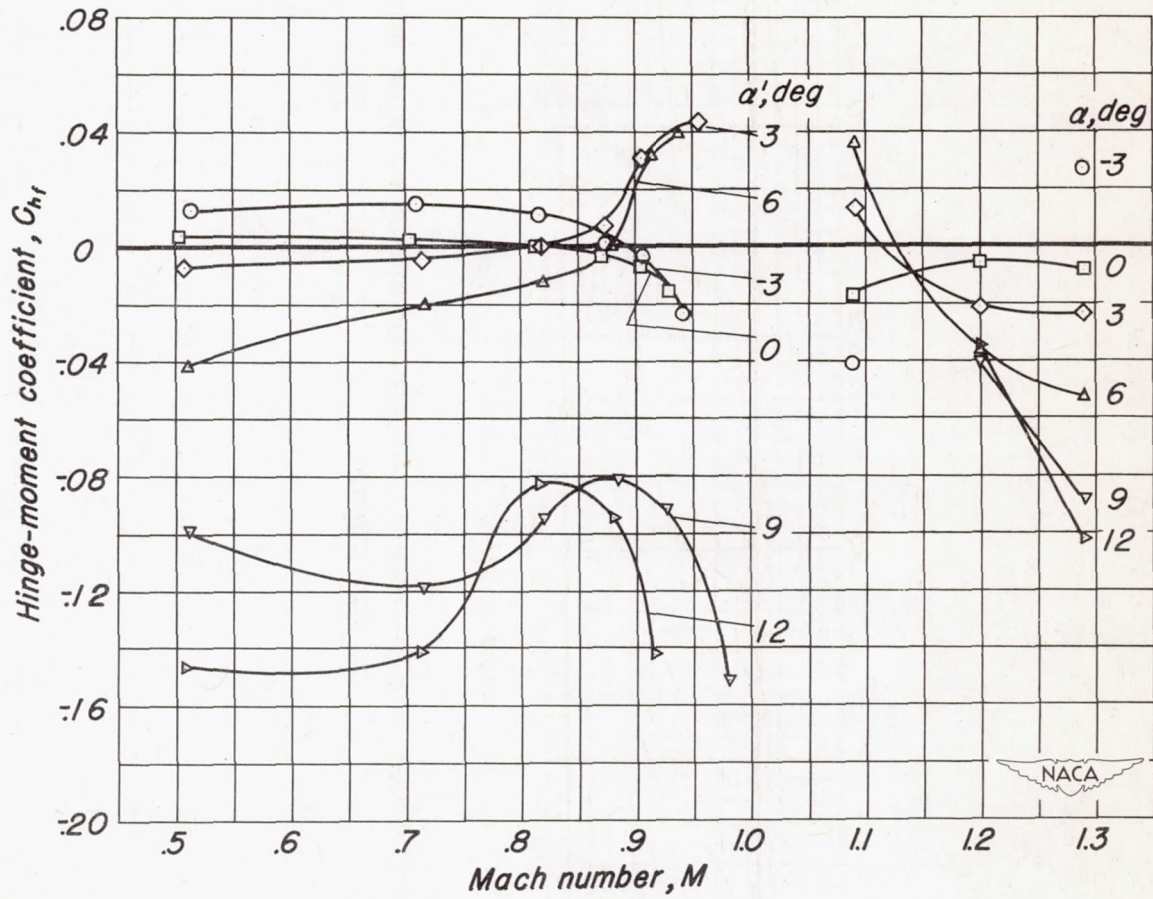
Figure 10.— Variation with Mach number of the hinge-moment coefficient of the trailing-edge flap for various geometric angles of attack; flaps undeflected, gaps unsealed.
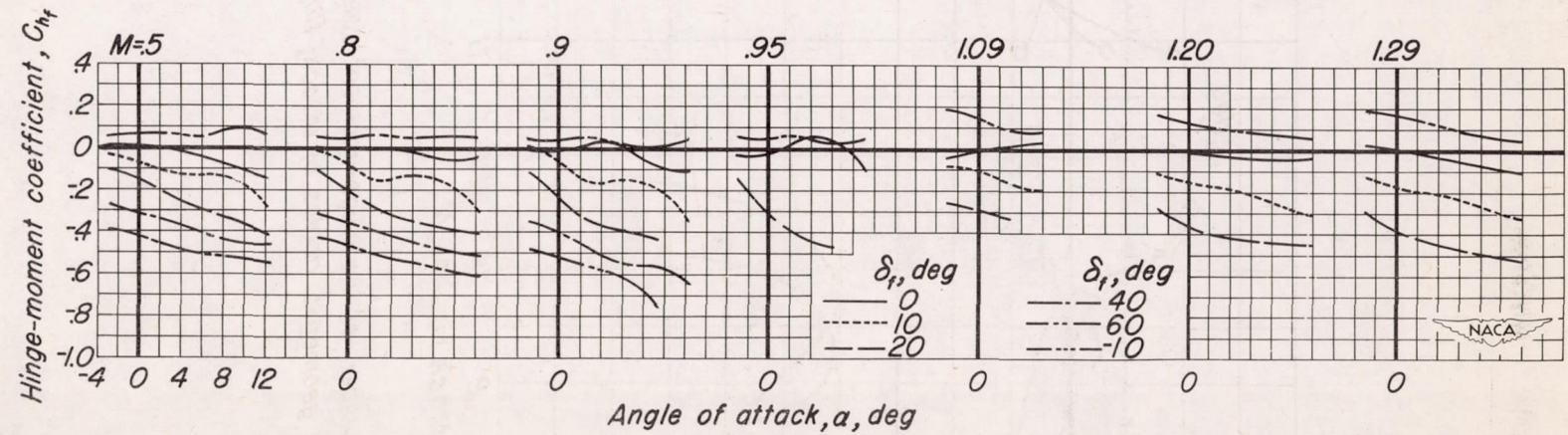
Figure 11.— Variation at several Mach numbers of hinge—moment coefficient with angle of attack for various flap deflections, gaps unsealed.
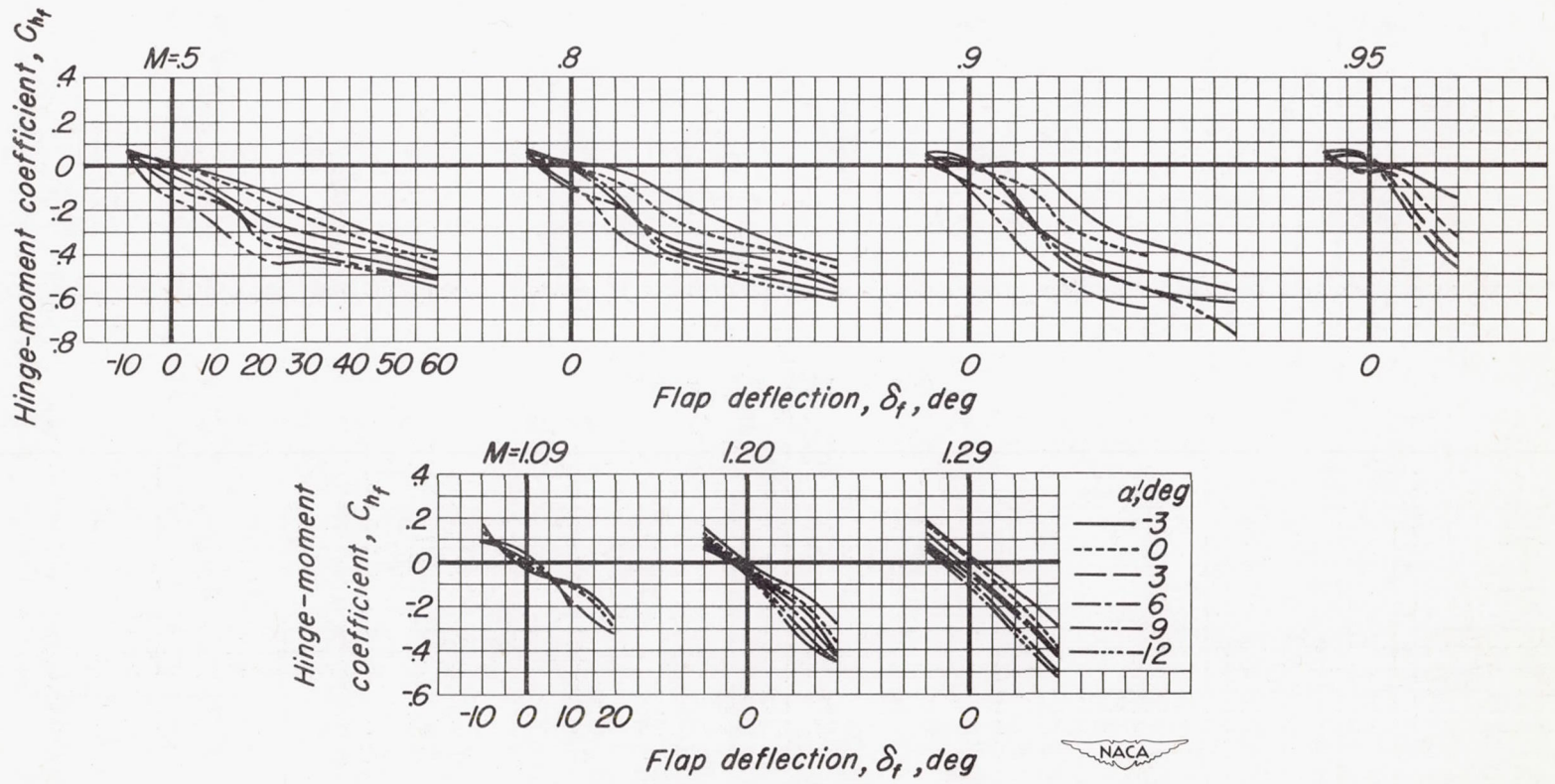
Figure 12.— Variation at several Mach numbers of hinge-moment coefficient with flap deflection for various geometric angles of attack, gaps unsealed.
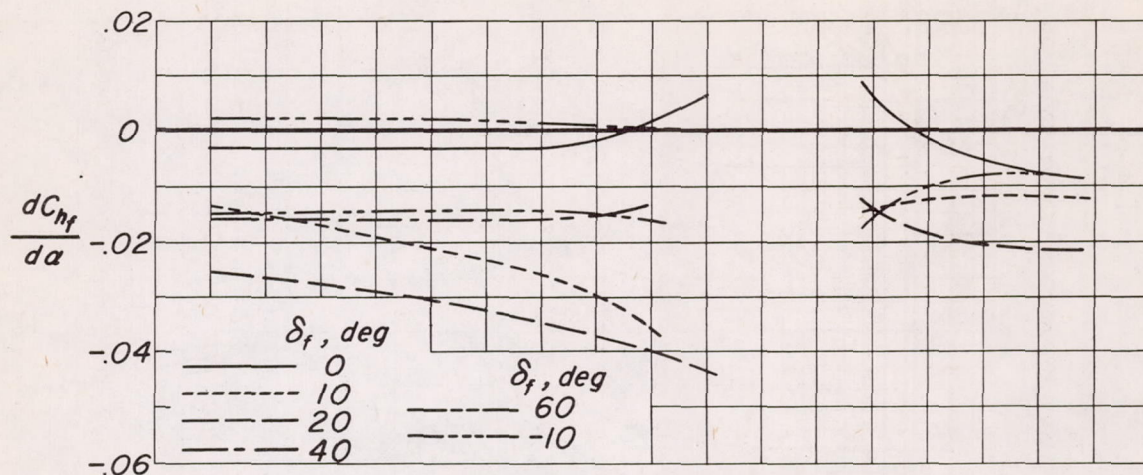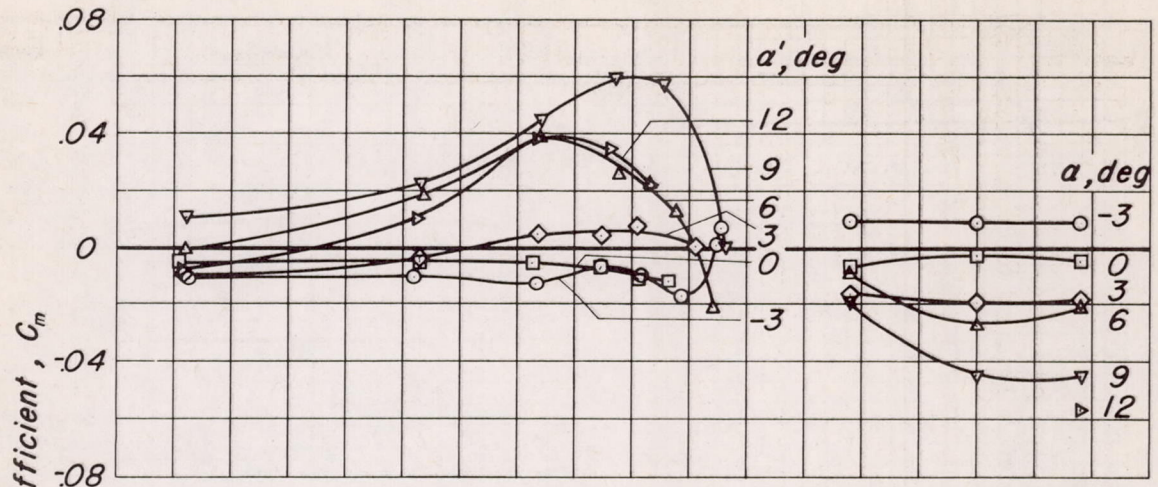
(a) Rate of change of hinge-moment coefficient with angle of attack at zero angle of attack.
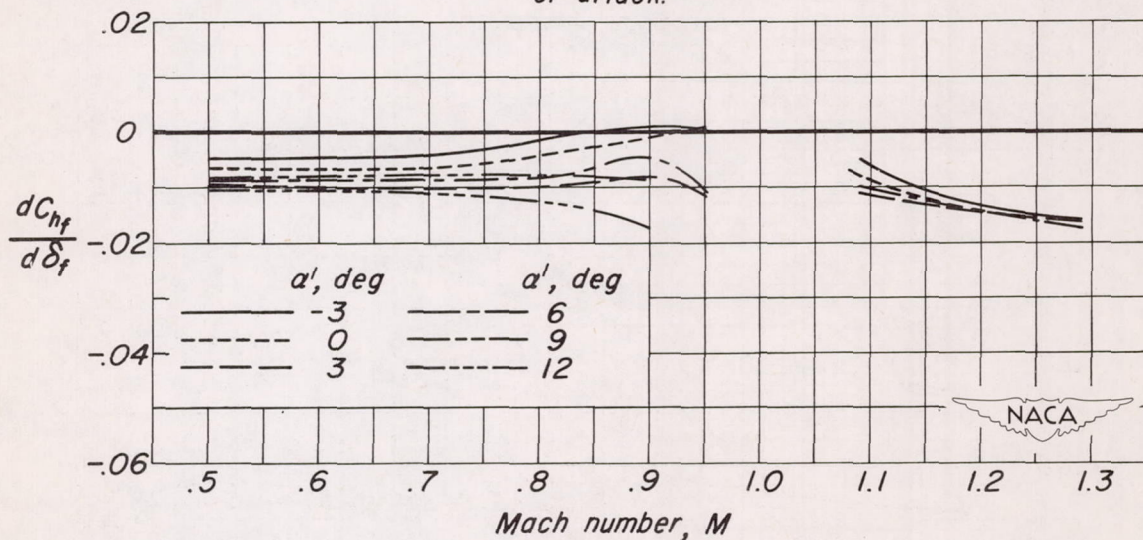
(b) Rate of change of hinge-moment coefficient with trailing-edge flap deflection at 0° deflection.

Figure 13.— Effects of Mach number on the slopes of the trailing-edge-flap hinge-moment curves, gaps unsealed.
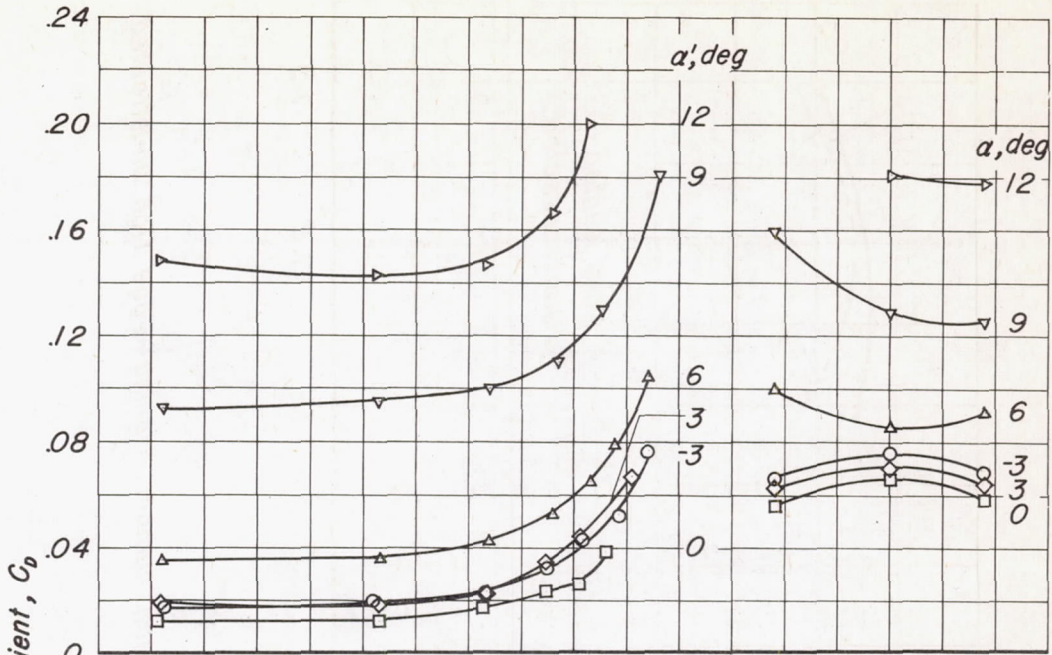
(a) Gaps unsealed.
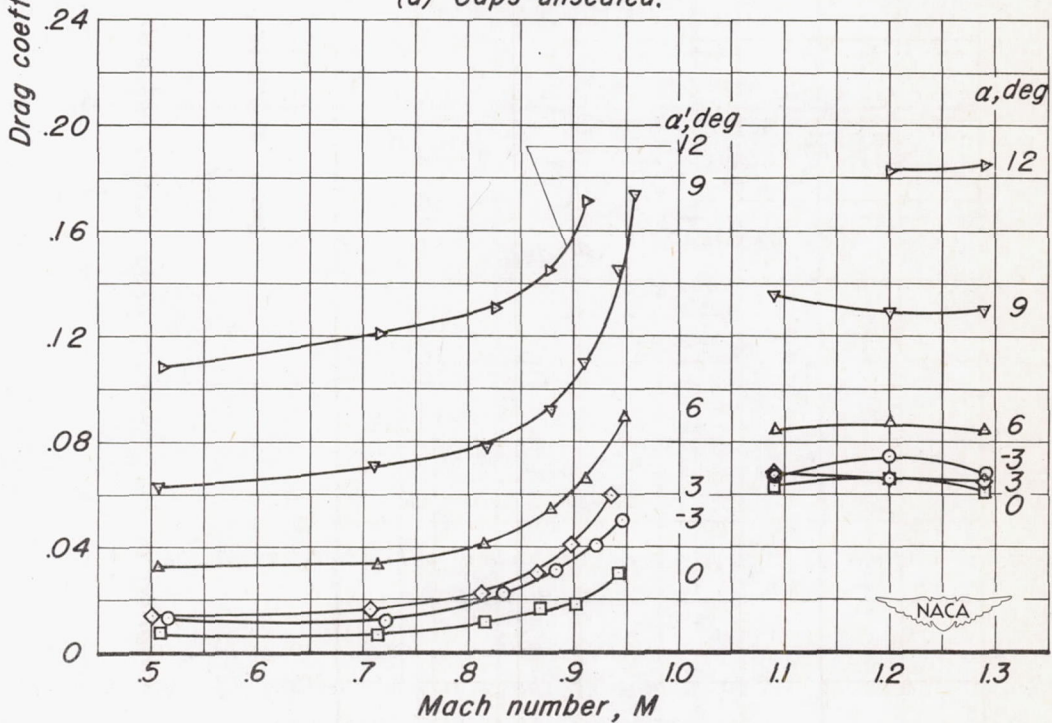
(b) Gaps sealed.

Figure 14.— Variation of drag coefficient with Mach number for various geometric
angles of attack, flaps undeflected.

Figure 15.— Variation of the minimum drag coefficient with Mach number, trailing-edge flap undeflected.

(a) Gaps unsealed.

Figure 16.— Variation at several Mach numbers of the drag coefficient with lift coefficient for various trailing—edge flap deflections.
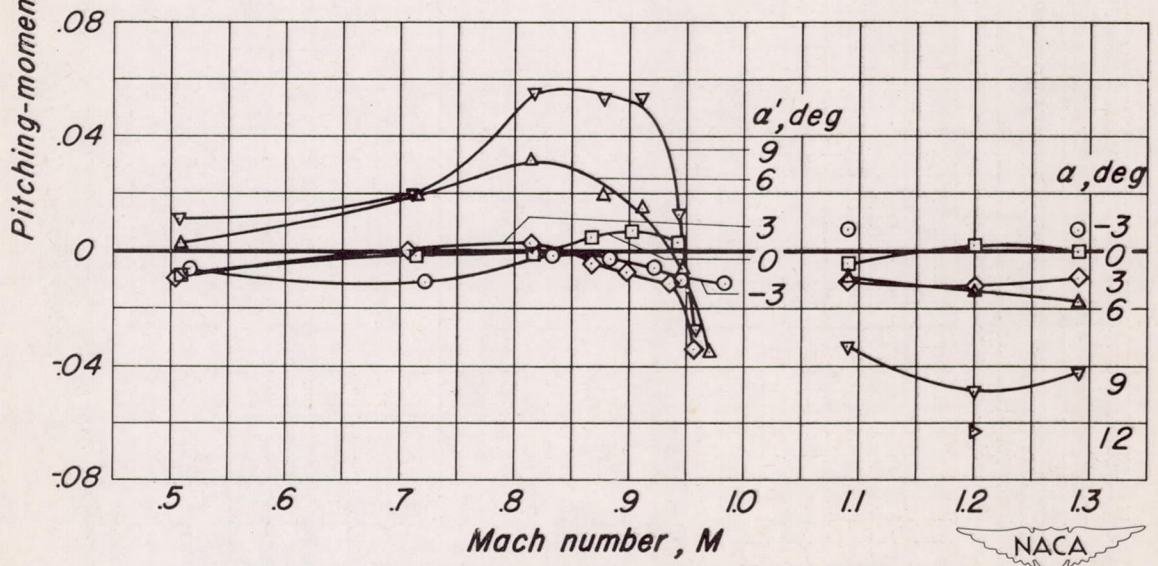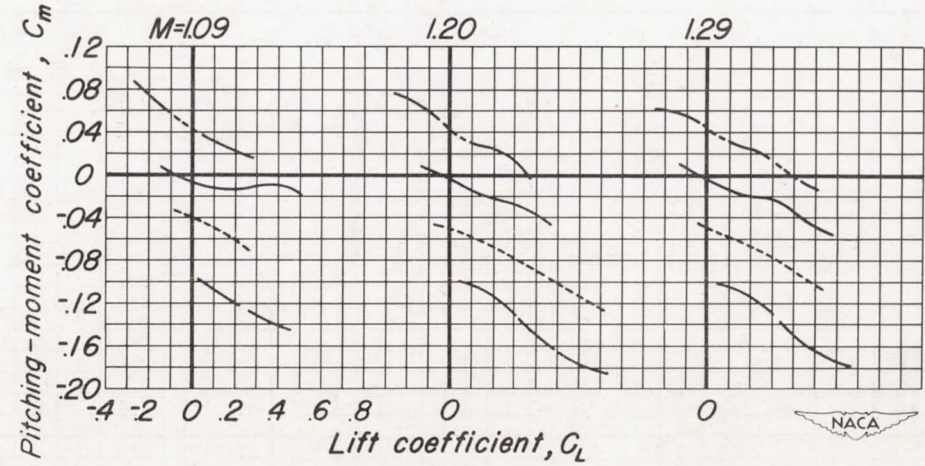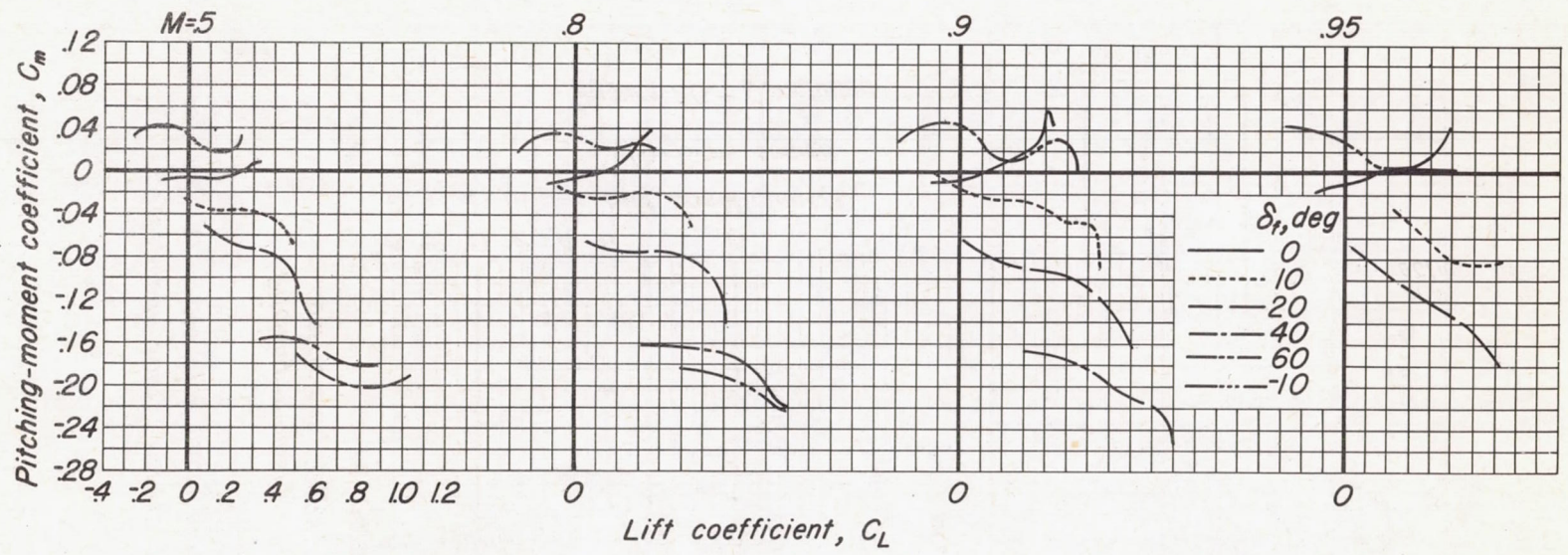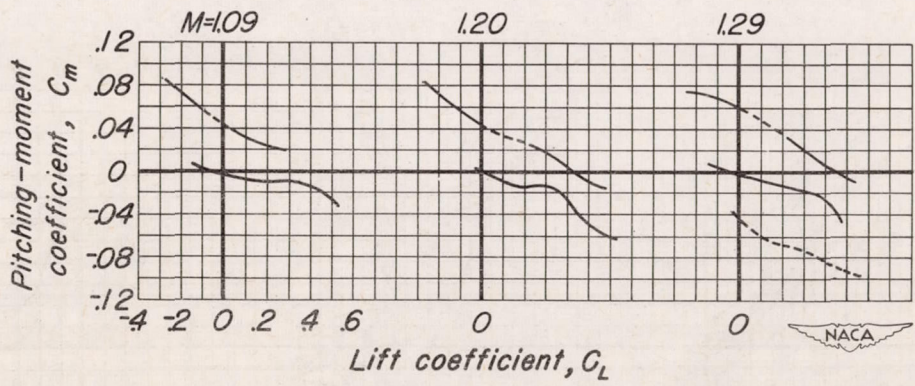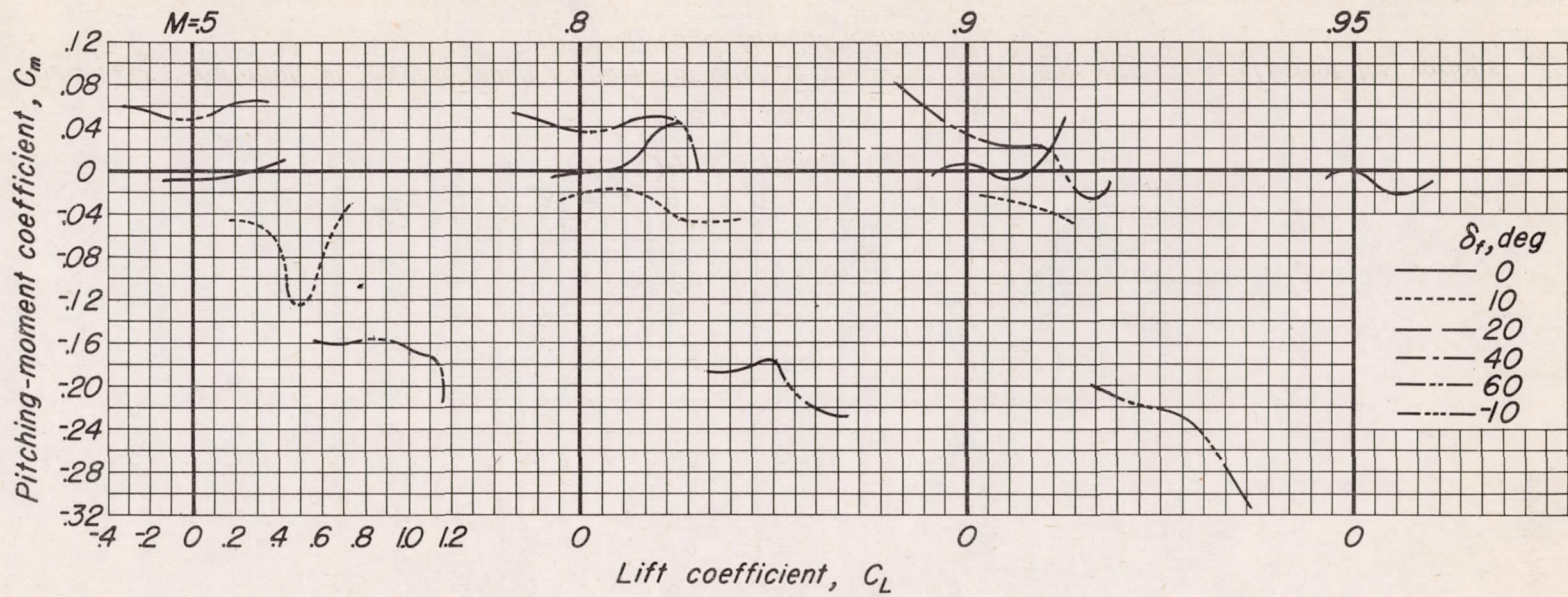
(b) Gaps sealed.

Figure 16.— Concluded.

Figure 17.— Variation at several Mach numbers of the drag coefficient with trailing-edge flap deflection for various geometric angles of attack, gaps unsealed.

(a) Gaps unsealed.

Figure 18.— Variation at several Mach numbers of lift-drag ratio with lift
coefficient for several trailing-edge flap deflections.

(b) Gaps sealed.

Figure 18.— Concluded.

Figure 19.— Variation of pitching—moment coefficient with Mach number for various geometric angles of attack, flaps undeflected.

(a) Gaps unsealed.

Figure 20.— Variation at several Mach numbers of pitching-moment coefficient with lift coefficient for various trailing-edge flap deflections.
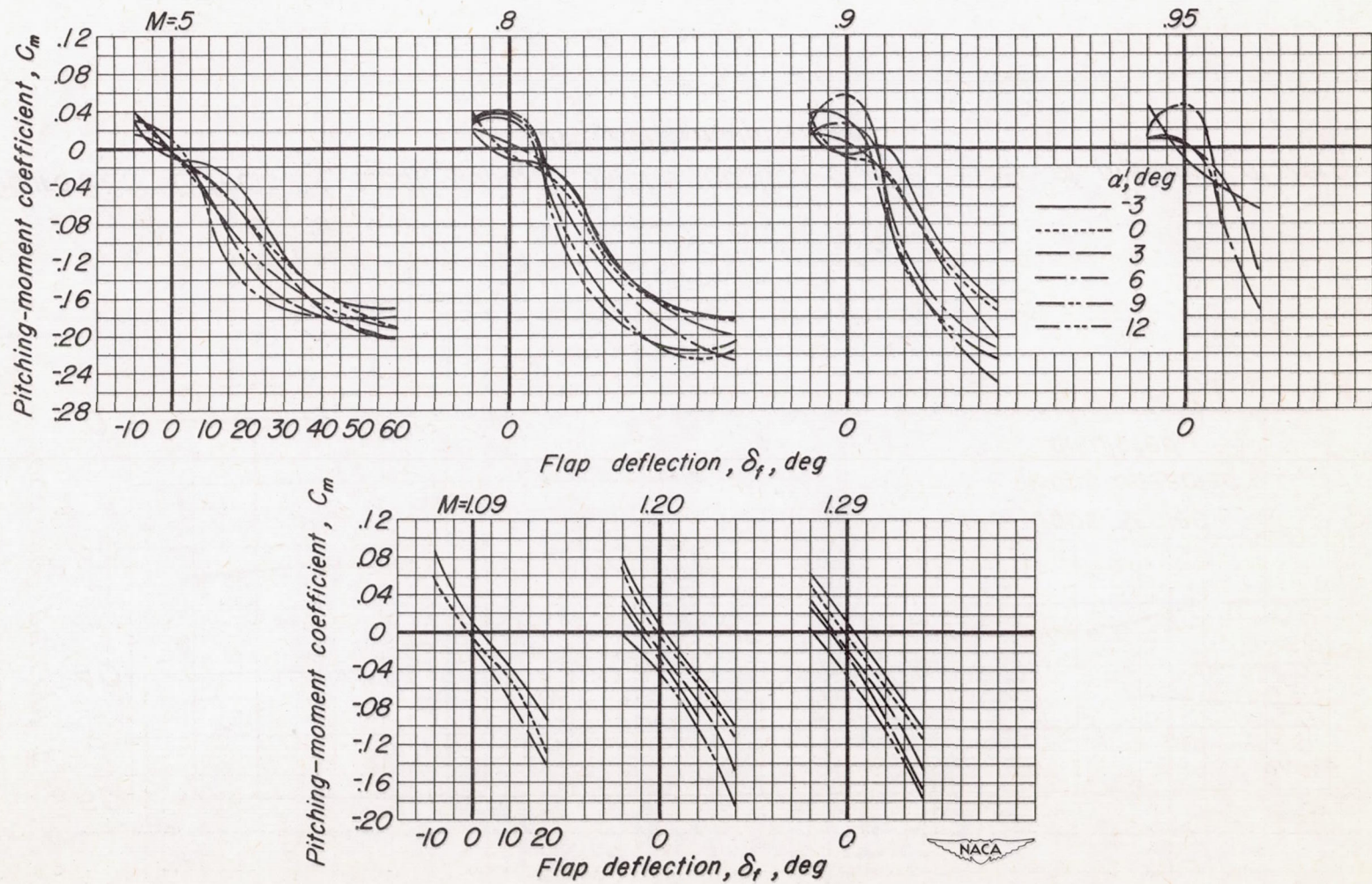
(b) Gaps sealed.

Figure 20.— Concluded.

Figure 21.— Variation at several Mach numbers of pitching-moment coefficient with trailing-edge flap deflection for several geometric angles of attack, gaps unsealed.
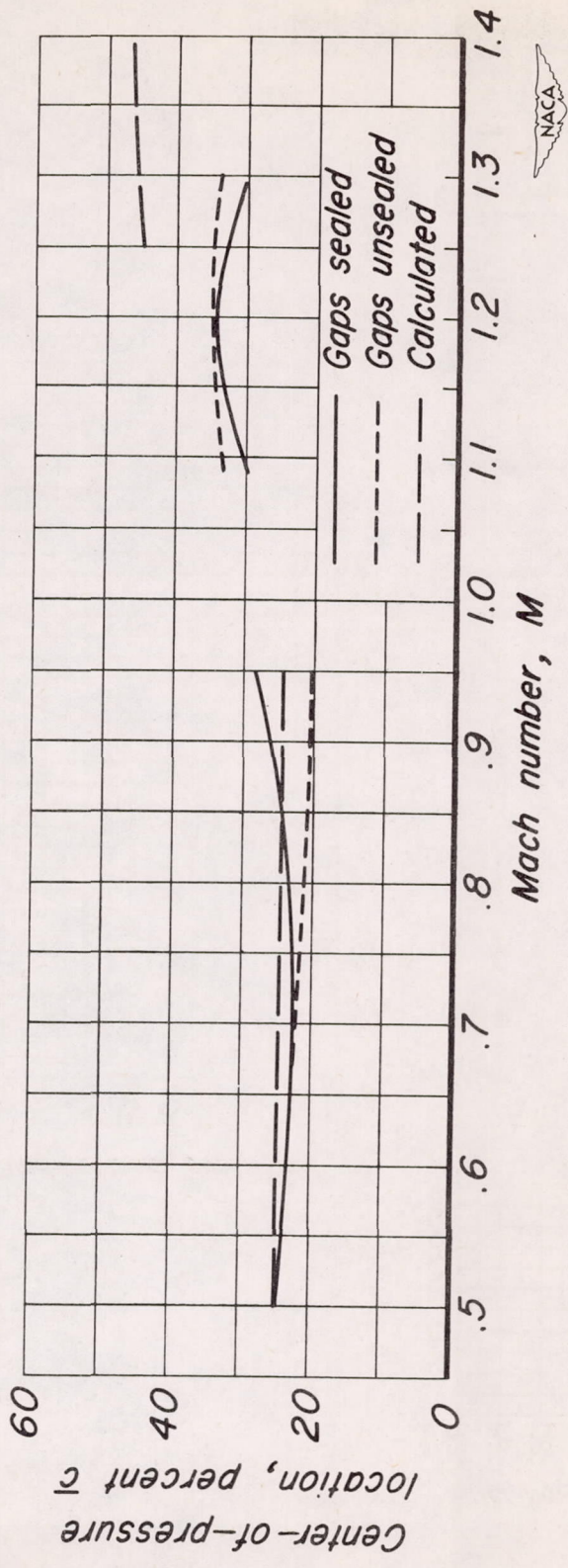
Figure 22.— Effects of Mach number on the location of the center of pressure at zero lift, flaps undeflected.